Geoderma 449 (2024) 117012

Contents lists available at ScienceDirect

Geoderma

journal homepage: www.elsevier.com/locate/geoderma

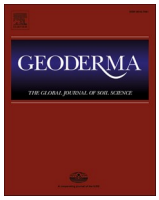

Applicability of calibrated diffuse reflectance spectroscopy models across spatial and temporal boundaries

Naveen K. Purushothaman [a], Kaushal K. Garg [b], A. Venkataradha [b], K.H. Anantha [b], Ramesh Singh [b], M.L. Jat [b], Bhabani S. Das [a,*]

[a] Agricultural and Food Engineering Department, Indian Institute of Technology Kharagpur 721302, West Bengal, India
[b] International Crops Research Institute for the Semi-Arid Tropics, Patancheru 502324, Telangana, India

ARTICLE INFO

Keywords:
Chemometric models
Smallholder farms
Soil test crop response rating
Spiking
Localizing

ABSTRACT

Diffuse reflectance spectroscopy (DRS) is an emerging soil testing approach. Although several studies have validated the DRS approach, limited efforts are made to assess the applicability of calibrated DRS models on new samples collected at different locations and/or time. To test such spatio-temporal applicability of calibrated DRS models, we collected surface soil samples from 1,112 smallholder farms during 2018 (T_{2018}) and 607 farms during 2021 (T_{2021}) covering seven districts of the Bundelkhand region of central India. The T_{2018} samples covered 7 development blocks; the T_{2021} samples were also collected from these blocks but from different sampling locations. Additionally, a new sampling site (Jhansi-Bamour block) was added during 2021 to create an independent test dataset. Collected samples were analysed for 17 soil parameters (basic soil properties, macronutrients, and micronutrients) and spectral reflectance over the visible to near-infrared region. Corresponding soil test crop response (STCR) ratings were also estimated. The Cubist model was calibrated in the T_{2018} dataset and tested against the T_{2021} dataset using the coefficient of determination (R^2), root-mean-squared error (RMSE), and percentage relative error deviation (PRED) at 30% error threshold as performance statistics. Model applicability was assessed at each block level (site-specific), by dividing the study site into their two geology-specific regions, and by treating the entire dataset as a regional-scale spectral library. Results showed that DRS models calibrated on a finer scale (site-specific) are less efficient in estimating soil parameters in broader scale (geology-specific and regional-scale) test T_{2021} samples although their STCR ratings may safely be estimated at local scales. When site-specific data were aggregated to broader scales and T_{2018} dataset was spiked with 20% samples from the T_{2021} dataset, model performance improved for critical soil parameters such as soil organic carbon (SOC) contents and several plant nutrients and their ratings; application of such large-scale models also improved the estimation accuracy when applied to site-specific datasets. Exchangeable Ca and Mg, clay and SOC contents were frequently well-estimated with R^2 values ranging from 0.54 to 0.93. Fine sand was the next best estimated soil property with R^2 values in the range of 0.40–0.75. The STCR ratings estimated in the DRS approach matched the wet chemistry-based STCR ratings to the tune of 43 to 100%. Overall, as many as 60% of all new samples could be estimated with more than 70% accuracy for 8 out of 17 parameters. With the DRS approach tested on both spatially- and temporally-independent test datasets and, specifically, with high estimation accuracy of STCR ratings, our results suggest that the DRS approach may safely be used as a viable alternative to conventional soil testing in smallholder farms.

1. Introduction

Soil health is increasingly considered as a key driver in tackling the global challenges of ensuring food security (Oliver and Gregory, 2015; Bagnall et al., 2021), alleviating malnutrition (Lal, 2017), combating climate change (Lal, 2011; Leal Filho et al., 2023), and achieving sustainable development goals (Lal et al., 2021). These challenges are particularly pronounced in arid and semi-arid regions where land degradation poses a significant problem (UNCCD, 2016; Jiang et al., 2020). The depletion of almost 66 % of carbon stored in plants and soil

* Corresponding author.
E-mail addresses: kaushal.garg@icrisat.org (K.K. Garg), venkataradha.akuraju@icrisat.org (A. Venkataradha), anantha.kanugod@icrisat.org (K.H. Anantha), ramesh.singh@icrisat.org (R. Singh), mangilal.jat@icrisat.org (M.L. Jat), bsdas@agfe.iitkgp.ac.in (B.S. Das).

https://doi.org/10.1016/j.geoderma.2024.117012
Received 28 February 2024; Received in revised form 20 August 2024; Accepted 20 August 2024
Available online 25 August 2024

over the last century because of land degradation clearly suggests the severity of the issue (Ekka et al., 2023). Soil-induced land degradation may be identified by slow and gradual decline in soil quality in terms of several physical, chemical, and biological properties that are known to be influenced by changes in land management practices (Rickson et al., 2012). Although regular soil testing is essential for guiding effective soil management practices (Havlin et al., 2014), soil testing itself is a challenge in many developing countries because of fragmented landholdings. As many as 475 million out of 570 million agricultural farms worldwide are smallholder farms (Nature Editorial, 2020). Most of these farms lack proper access to essential agricultural inputs (Ricciardi et al., 2021) and necessary agricultural technologies (Laborde et al., 2020; Nature Editorial, 2020). Reversing land degradation in such resource-poor agricultural systems requires rapid and adequate assessment of the existing soil health status. The conventional wet chemistry method of testing soils remains expensive and time-consuming.

Soil health is a composite soil attribute (Allen et al., 2011), which requires several soil parameters to be measured for a given sample and over the region of interest. The requirement for the so-called 3H data of High accuracy, High spatial resolution, and High spatio-temporal continuity (Huang et al., 2022) for multiple soil parameters makes soil health assessment a daunting task specifically when wet chemistry-based (conventional) soil testing methods are followed (Viscarra Rossel et al., 2006). Over the past few decades, diffuse reflectance spectroscopy (DRS) is emerging as an alternative for conventional soil testing (Ben-Dor and Banin, 1995; Viscarra Rossel et al., 2016; Li et al., 2022b). Several experimental assessments (Reeves et al., 1999; Wang et al., 2012; Tian et al., 2013), extensive reviews (Bellon-Maurel et al., 2010; Ahmadi et al., 2021), and farm-scale assessment of DRS approaches (Rodionov et al., 2015; Franceschini et al., 2018) have comprehensively shown that multiple soil parameters (Table S1) may be estimated using the DRS approach both in the proximal (Majeed et al., 2023a) and remote (Majeed et al., 2023b) sensing modes even in smallholder farms. Moreover, the DRS approach yields similar nutrient recommendations (Singh et al., 2019; Zeng et al., 2022; Majeed et al., 2023a). Singh et al. (2019) showed that both the conventional and DRS-based soil testing yielded similar nutrient ratios for making balanced nutrient applications to the cocoa production systems. Because farmers generally apply nutrients based on soil test crop response (STCR) ratings derived from soil test results, Zeng et al. (2022) estimated these ratings for 20 soil indicators directly from soil spectra while Majeed et al. (2023a) obtained similar STCR ratings from conventional and DRS-based soil test results for 14 different soil indicators. These studies suggest that DRS approach may be directly used in production agriculture from a precision farming standpoint.

The DRS approach is cost-effective when high through-put sample testing is needed such as those required in many smallholder farms of developing countries. Studies have shown that the DRS approach is less costly when a large number of samples have to be analysed (Li et al., 2022b). Rapid and cost-effective soil testing with the DRS approach will also enable easy spatial soil assessment through geospatial methods such as kriging and digital soil mapping approaches (Viscarra Rossel and McBratney, 2008; de Souza Bahia et al., 2017). Despite these advantages, DRS approach as a viable alternative to wet chemistry-based soil testing is debated (McBride, 2022; Viscarra Rossel et al., 2022). The primary reason behind such a debate is the accuracy and, to some extent, the cost of the DRS technology. The accuracy of the DRS approach depends on several factors such as the size of calibration samples (Guerrero et al., 2010; Lucà et al., 2017), spatial scales (Gomez and Coulouma, 2018), modelling approaches (Liu et al., 2018), soil pre-processing approaches (Brunet et al., 2007), and soil heterogeneity (Lobsey et al., 2017; Zayani et al., 2023) among others. Viscarra Rossel et al. (2022) suggest that the use of a suitably sampled validation dataset may ensure reliable application of the DRS approach.

Global efforts in creating comprehensive spectral libraries, robust chemometric models, different modelling strategies, and varied pre-processing methods have significantly improved the performance of the DRS approach (Bellinaso et al., 2010; Viscarra Rossel et al., 2016; Ludwig et al., 2019; Wang and Wang, 2022). Many of these studies have critically dealt with the spatial aspects of having large areas in the analysis or having large spectral libraries with several samples in the calibration dataset. However, few studies have examined the temporal aspect of model assessment. Although temporal changes in soil properties may generally be slow (Zayani et al., 2023), aggressive agricultural practices and rapid land degradation processes may cause major changes in several soil properties such as soil reaction, soil physical characteristics, soil organic carbon (SOC) contents, and soil nutrient contents. With fewer DRS studies focused on testing a validated model in samples collected during different sampling periods, there is a need to evaluate the DRS approach in such newly collected samples.

The accuracy of a calibrated DRS model in estimating soil properties in new samples is a key challenge for the adoption of DRS approach as a viable alternative to conventional soil testing. The term 'new' encompasses various aspects including samples from the same region where the DRS model is calibrated, from the same location but at a different time, or from a different location and collected at a different time. Applicability of calibrated DRS models (Sudduth and Hummel, 1996; Grunwald et al., 2018) to estimate several soil parameters in new samples collected from different locations or at a different time than those of their calibration samples is relatively less studied. We identified four reported studies (Table 1) that dealt with applicability of trained DRS

Table 1
List of studies evaluated the applicability of trained reflectance spectroscopy models on the temporal dataset for estimating selected soil properties.

Attributes	Morais et al. (2021)	Barbetti et al. (2023)	Tsatsoulis et al. (2023)	Zayani et al. (2023)
Study area	Portugal	Northern Italy	European Union	France
Scale	Farm level	Regional and farm level	Continental level	Watershed level
Area (km^2)	1.26	–	~10 Million	12
Soil properties	SOC	SOC	SOC, sand, silt, clay, and pH	SOC
Number of samples	2018: 137 2019: 36	2003: 54 2012: 54 2018: 54 Regional-SSL: 122	2009: 17,937 2015: 20,687	2013: 394 2018: 111
Chemometric models	ANN	RF, Cubist, MBL	PLSR and RF	PLSR
Spiking method	–	–	10 % of 2015 samples selected using KS algorithm and augmented with 2009 dataset	10 % of 2018 samples selected randomly and augmented with 2013 dataset
Modelling scenarios	Leave one farm and one-year cross validation	a) Local-SSL b) Regional-SSL	a) Cross year testing (2009 train and 2015 test) b) Spiking	a) Without spiking b) Spiking
Performance statistics (R^2)	0.24 - 0.88	a) 0.79 - 0.87 b) 0.78 - 0.87	a) SOC: 0.61 - 0.68, Clay: 0.50 - 0.57 b) SOC: 0.70, Clay: 0.55 - 0.59	a) 0.44 - 0.84 b) 0.65 - 0.85

SOC: soil organic carbon; SSL: soil spectral library; ANN: artificial neural network; RF: random forest; MBL: memory-based learning; PLSR: partial-least-square regression; R^2: coefficient of determination.

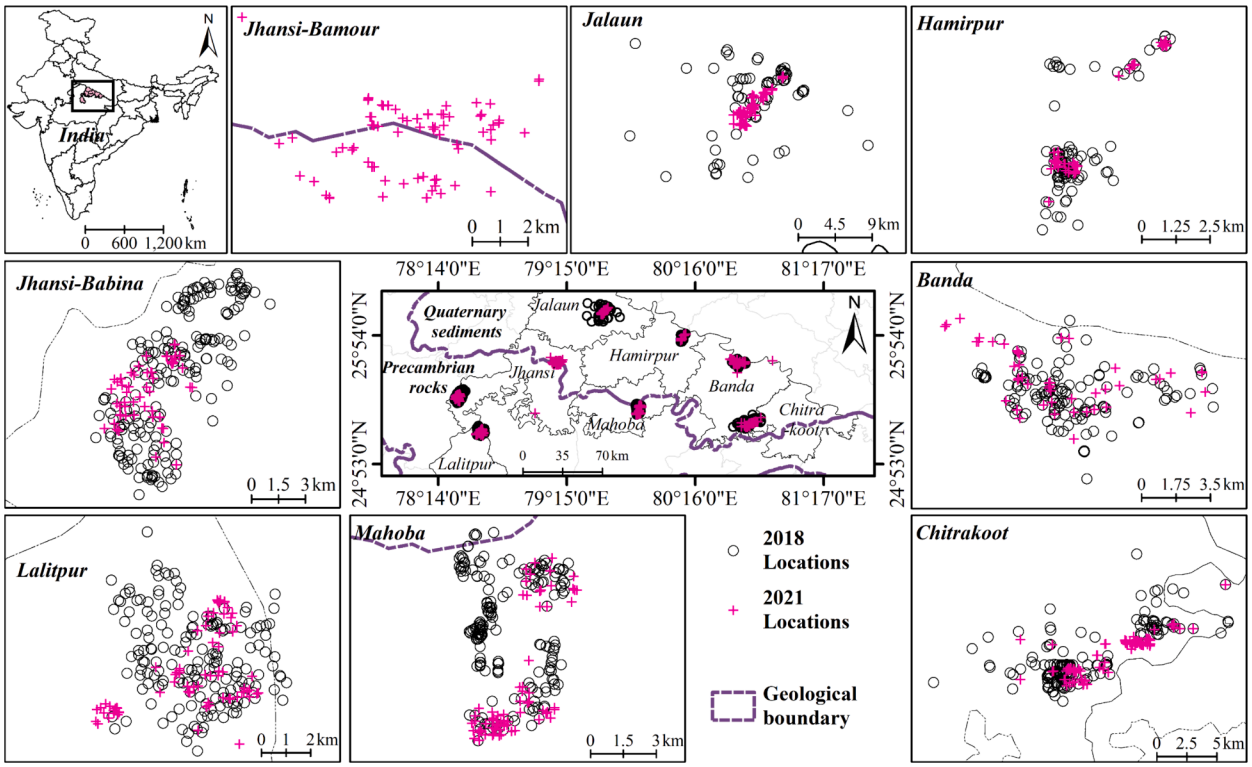

Fig. 1. Locations of soil samples collected from selected districts of Bundelkhand region during 2018 (open circles) and 2021 (plus sign).

models on the temporal dataset. These studies primarily focused on estimating SOC contents; textural fractions and soil pH were included only in Tsatsoulis et al. (2023). The applicability of the trained DRS models on the temporal dataset for a suite of soil parameters generally included in conventional soil testing has not been well reported in the literature. Moreover, existing studies generally involved the collection of samples from the same locations (or farms) precluding the assessment of spatio-temporal applicability of DRS models. The temporal localizing of regional models to site-specific scales has also not yet been explored. While critical studies on the applicability of trained DRS models are limited, the DRS literature generally does not address a commercial aspect of DRS model testing in line with how many new samples can be tested with predefined error tolerance.

Our primary goal is to evaluate the applicability of calibrated DRS models using spatially- and temporally-independent test datasets. Specifically, our goal is to find the fraction of accurately estimated new samples using pre-calibrated DRS models. Studies also have shown that a subset of these new samples be analysed through conventional soil testing methods and added to the existing calibration data to achieve improved accuracy using a recalibrated model from such spiked calibration data (Ng et al., 2022; Zayani et al., 2023). Thus, the second objective of our study is to identify which of these new samples best-suited for spiking. Furthermore, because the purpose of soil testing in smallholder farms is to make nutrient recommendations, the third objective of this study is to test whether a well-calibrated DRS model can yield similar STCR ratings as their wet chemistry-based estimates.

2. Materials and methods

2.1. Study area and soil sampling

The study site comprised seven districts (Jhansi, Jalaun, Lalitpur, Mahoba, Hamirpur, Banda, and Chitrakoot) of the Uttar Pradesh state, which form a major part of the Bundelkhand region in Central India (Fig. 1). Developed on the Bundelkhand craton, the region has two distinctive geology with Indo-Gangetic alluvium concealing the northern part of the craton and the Precambrian crust rich in granite-gneiss on the south (Sharma and Mondal, 2019). The dashed line (Fig. 1) shows the geological boundary separating Lalitpur, Jhansi and Mahoba districts (Precambrian rocks) from the remaining districts dominated by the quaternary sedimentary rocks (Wandrey and Law, 1997). With both sedimentary and igneous rock systems, soils of the Bundelkhand region are diverse and are classified under either Entisols, Alfisols, Inceptisols, or Vertisols (Kumar et al., 2021).

Bundelkhand region has a semi-arid climate and relies heavily on rainfed agriculture. Annual rainfall ranges from 550 to 800 mm with large spatial and temporal variations across the region (Singh et al., 2022). Maximum summer temperatures often exceed 45–47 °C while temperature could drop below 4 °C during winter months of December and January (Kumar et al., 2021). About 52 % of the total cultivable area in this region relies solely on rainfall for agricultural sustenance (Kumar et al., 2021). Droughts, erratic rainfall, frequent dry spells, water scarcity, poor soil quality, and soil erosion are some of the major challenges to rainfed farming in this region (Jatav, 2022; Majeed et al., 2023a). Prominent *kharif* crops (grown during rainy season) include groundnut (*Arachis hypogaea*), black gram (*Vigna mungo*), green gram (*Vigna radiata*), sesame (*Sesamum indicum*), and pigeon pea (*Cajanas cajan*) while *rabi* crops (grown during winter season) include mustard (*Brassica juncea*), chickpea (*Cicer arietinum*), field pea (*Pisum sativum*), barley (*Hordeum vulgare*), and wheat (*Triticum aestivum*) (Singh et al., 2022). Wasteland often covers as much as 20 % of the total geographical area of this region (Majeed et al., 2023a).

The International Crop Research Institute for the Semi-Arid Tropics (ICRISAT), Patancheru, Hyderabad implemented a mesoscale land rehabilitation project in these districts (Garg et al., 2020). Based on diverse soil types, topographies, land uses, and cropping systems, a stratified sampling approach was followed to select smallholder farms for collecting soil samples during two sampling campaigns. The first set of surface soil samples (0–15 cm depth) were collected during May-June 2018 (T_{2018}) from 1,112 smallholder farms from 20 villages distributed

over 7 development blocks (Table S2) of the selected districts. The second soil sampling campaign was conducted during March-April 2021 (T_{2021}) in the same 20 villages but from randomly selected 607 smallholder farms that were different from T_{2018} sampling. For the Jhansi district, surface soil samples were also collected from 98 selected smallholder farms covering two new villages (Sutta and Singar) of Bamour development block (hereinafter, referred to as Jhansi-Bamour site) during 2021 in addition to the existing Babina block (hereinafter, referred to as Jhansi-Babina site) of T_{2018} dataset. With no soil samples collected from this site during 2018, the Jhansi-Bamour site served as both spatially-independent (i.e., outside the sampling region of T_{2018} samples) and temporally-independent (e.g., no soil samples were collected during 2018) test dataset for the evaluation of the DRS approach.

2.2. Measurement of soil properties and collection of soil spectra

Collected soil samples were air-dried, ground, sifted through 2 mm sieve, and analysed using standard soil testing procedures. Each sample was analysed for 17 soil parameters: 3 soil textural fractions (coarse sand, fine sand, and clay contents), pH, SOC content, electrical conductivity (EC), exchangeable Na, and 10 plant nutrients (P, K, Ca, Mg, S, Fe, Mn, Cu, Zn, B). Soil texture was analysed using the hydrometer method (Sarkar and Haldar, 2005). Soil pH and EC was measured in 1:2 and 1:2.5 soil:water slurry, respectively. The SOC content was estimated using the chromic acid digestion method (Walkley and Black, 1934). Available P was estimated using the Olsen's and Bray's method using a continuous auto-analyser (Olsen and Sommers, 1982). The ammonium acetate method was used to extract available cations such as Ca, Mg, Na, and K (Hanway and Heidel, 1952). A flame photometer (Systronics India Ltd., Ahmedabad, India) was used to measure exchangeable cation concentrations. Micronutrients such as Fe, Mn, Cu, and Zn were analysed using the diethylenetriamine penta-acetic acid (DTPA) extraction method and an inductively-coupled plasma spectrometer (Model: HD prodigy; Teledyne Leeman Labs, USA). The hot-water extraction method was followed for available B (Keren, 1996). The similarity between soil properties from T_{2018} and T_{2021} datasets was assessed using the Wilcoxon rank sum test built in the *stats* package of R Studio (ver. 4.3.1; R Core Team, 2023). We also estimated the STCR ratings using the three-tier STCR classification scheme (Table S3) generally used for Indian soils (Sendhil et al., 2018). Because the STCR ratings (threshold values) for soil textural fractions and exchangeable Na are not available, we estimated the STCR ratings for the remaining 13 soil parameters using their laboratory-measured values in each soil sample.

Spectral reflectance data of processed soil samples were collected in a proximal mode over the visible to near-infrared (VNIR) region (wavelength: 350–2,500 nm) using a portable spectroradiometer (Model: Field spec®4 Hi-Res NG; Malvern Panalytical Ltd., USA). A turntable fitted with a halogen bulb as its light source was used to collect spatially-averaged reflectance spectra for repacked soil samples. About 100 g of processed soil sample was used to completely fill the glass petri dish, and the soil surface in each petri dish was leveled using a thin glass plate (to avoid soil compression in the petri dish). The Spectralon® white reference panel (Lab sphere, USA) was used to obtain a reference spectrum. Soil spectra were collected following the standard protocol of a) warming up the instrument for 1 h before data collection, b) optimization for the light source and the collection of white reference spectra after every 30 samples, and c) averaging of 30 scans per sample. Each spectrum was clipped to retain the reflectance values in the range of 400 nm to 2450 nm. Each reflectance value was then transformed to absorbance. Smoothing of individual spectra was done by a second-order Savitzky-Golay smoothing method (Savitzky and Golay, 1964) with the span length of 11 nm to remove noise for optimizing the signal-to-noise ratio (Ng et al., 2019b; Viscarra Rossel et al., 2024). Resulting absorbance spectra was then resampled at 10 nm interval to reduce collinearity (Viscarra Rossel and Webster, 2012; Luce et al., 2022). A standard normal variate (SNV) transformation was then applied to each spectrum to reduce the effect of light scattering (Barnes et al., 1989). All pre-processing steps were performed using the *prospectr* package (version 0.2.6; Stevens and Ramirez-Lopez, 2022) with R studio version 4.3.1 software (R Core Team, 2023).

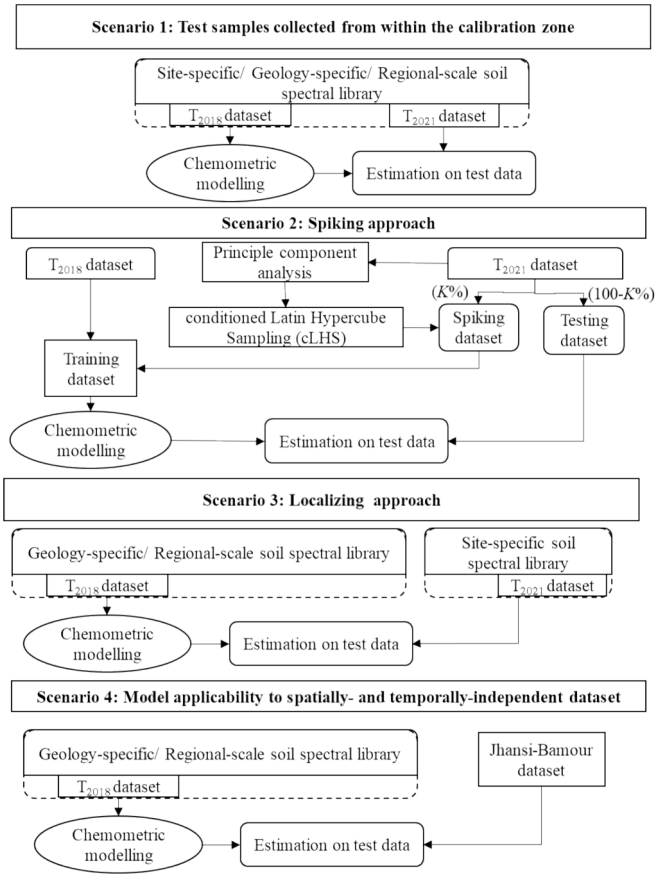

Fig. 2. Flowchart of different scenarios examined for the spatio-temporal applicability of calibrated models.

2.3. Assessment of DRS model applicability for estimating soil parameters and their ratings

The applicability of DRS models for estimating soil parameters and their STCR ratings was evaluated by calibrating a suitable chemometric model and examining how such a model performs in new soil samples collected at a different time and at a different location than the calibration samples. We also evaluated the localizing aspect of the models wherein the information generated in a broader spatial scale was transferred to a finer spatial scale (Blöschl and Sivapalan, 1995; Wu et al., 2006).

2.3.1. Selection of chemometric model

Some of the recent DRS studies suggest that the Cubist (O'Rourke et al., 2016; Viscarra Rossel et al., 2016; Dangal et al., 2019; Zhao et al., 2024; Xu et al., 2024), feature selection-based PLSR (Ng et al., 2019a; Dorantes et al., 2022), support vector regression (Ahmadi et al., 2021), and memory-based learning algorithm (Ramirez-Lopez et al., 2013; Sanderman et al., 2023) perform more efficiently than other chemometric models for estimating soil properties in the DRS approach. These models were, therefore, compared to identify a single chemometric model to estimate all the 17 soil parameters such that a fair comparison may be made for the applicability of DRS approach across different soil parameters and different modelling scenarios. This preliminary analysis

suggested that the Cubist model had the best performance when calibrated using the pooled T_{2018} data and tested against those of the T_{2021} data. An extension of the M5 model tree, the Cubist model is a rule-based regression model (Quinlan, 1993), which was introduced as an alternative to commonly used chemometric models for estimating soil parameters in the DRS approach (Minasny and McBratney, 2008). The algorithm segments data with similar spectral characteristics and formulates one or more rules for each segment. Because the algorithm includes multiple interactions and both linear and nonlinear correlations between VNIR data and soil properties (Minasny et al. 2011), Cubist generally outperforms other competitive models, as may also be seen from higher coefficient of determination (R^2) values in Fig. S1. Therefore, we used the Cubist model for the remainder of our data analyses.

We followed a two-step procedure to assess the applicability of the calibrated DRS models. Initially, a ten-fold cross-validation was applied to the T_{2018} dataset to develop chemometric models and tune hyperparameters to avoid overfitting issues. Then the cross-validated models were tested on the T_{2021} dataset to quantify their performance on new soil samples. The Cubist model was implemented in R (version 4.3.1; R Core Team, 2023) using the *cubist* package (version 0.4.2.1; Kuhn and Quinlan, 2023). Optimization involved a ten-fold cross-validation approach on the training dataset by employing a grid search via the *caret* (version 6.0–94; Kuhn, 2008) package in R. The performance of the model was enhanced by optimizing two parameters of committees and neighbours. Committees were varied from 1 to 100 with intervals of 10, while neighbours were explored from 0 to 9 with intervals of 1 (Coblinski et al., 2020).

2.3.2. Scenarios for assessment of the applicability of trained DRS models

Four modelling scenarios were considered to evaluate the efficacy of chemometric models for estimating each soil parameter and its STCR ratings in independent test samples of T_{2021} (Fig. 2).

In scenario 1 (test samples collected from within the calibration zone), soil parameters were estimated by calibrating a chemometric model using the T_{2018} dataset and then testing the resulting model on the T_{2021} dataset. Three cases were considered under this scenario: site-specific, geology-specific, and the regional-scale:

- Site-specific calibration: chemometric models for each soil parameter were calibrated using the district-wise data of the T_{2018} and the developed model was tested against their respective T_{2021} datasets.
- Geology-specific calibration: soil samples from the Lalitpur, Jhansi-Babina, and Mahoba were pooled to construct the training (T_{2018}) and testing (T_{2021}) datasets with Precambrian crust geology (PCG). Similarly, soil samples from the remaining districts were pooled to construct respective training and testing datasets with the quaternary sediment geology (QSG). Because soil samples from Jhansi-Bamour were distributed across both sides of this geological boundary and were not collected during 2018 sampling campaign, these samples were not included in the analysis.
- Regional calibration: samples collected during 2018 from all the districts were pooled together to calibrate regional-scale DRS models, which were then tested against the pooled datasets of T_{2021} (excluding Jhansi-Bamour dataset).

In scenario 2 (spiking approach), a subset of T_{2021} dataset was selected and added to the T_{2018} dataset to augment the training dataset with characteristic features of the T_{2021} dataset. Model assessment outlined in scenario 1 was then repeated using these augmented T_{2018} dataset as calibration data and the remainder of the T_{2021} dataset as test data. This approach is commonly referred to as spiking (Shepherd and Walsh, 2002; Ng et al., 2022). For selecting the spiking subset from T_{2021} dataset, the conditioned Latin hypercube sampling (cLHS) approach was followed (Minasny and McBratney, 2006) because of its effectiveness in selecting samples for spiking an existing calibration dataset (Ramirez-Lopez et al., 2014; Gholizadeh et al., 2018; Ng et al., 2018; Li et al., 2022a; Li et al., 2022b; Luce et al. 2022; Sanderman et al., 2023; Moloney et al., 2023; Yang et al., 2023). For implementing the cLHS approach, standardized principal component (PC) scores were obtained for the first four PCs estimated from T_{2021} soil spectra because these 4 PCs explained 99.99 % of the total variance in our dataset. The *clhs* package (ver. 0.9.0) from R Studio (ver, 4.0.5; R Core Team, 2023) was used to implement the cLHS algorithm (Roudier, 2011) with varying sample sizes (up to 50 % of the dataset).

In scenario 3 (localizing approach), the geology-specific and regional-scale models calibrated under the scenario 1 and scenario 2 were tested for each of the site-specific datasets. The DRS models calibrated using the geology-specific and regional-scale datasets (pooled data from multiple development blocks) were applied to estimate soil properties of specific sites (individual development block).

In scenario 4 (model applicability to spatially- and temporally-independent dataset), both the geology-specific and regional-scale models were tested on the Jhansi-Bamour dataset, which served as a spatially- and temporally-independent test dataset. Models calibrated with both before and after spiking T_{2018} data were used for this purpose. Scenario 4 represents the case of model applicability beyond spatial and temporal dimensions.

2.3.3. Assessment of prediction accuracy

Prediction accuracy of each chemometric model was assessed using the root-mean-squared error (RMSE) and R^2:

$$RMSE = \sqrt{\frac{\sum_{i=1}^{N}(Y_i - \widehat{Y}_i)^2}{N}} \tag{1}$$

$$R^2 = 1 - \frac{\sum_{i=1}^{N}(Y_i - \widehat{Y}_i)^2}{\sum_{i=1}^{N}(Y_i - \overline{Y})^2} \tag{2}$$

where Y_i is the measured soil parameter with its mean value of $\overline{Y}$ and predicted value of $\widehat{Y}_i$ at the i^{th} location and N is the number of locations. The bias values were also calculated as the difference between the mean value of predicted and measured soil properties. Other metrics such as range error ratio (RER), ratio of performance to deviation (RPD), and ratio of performance to interquartile range (RPIQR) values were also estimated. While these conventional metrices provide estimates of typical error associated with a specific prediction system (pre-processing approach and/or chemometric model), it is also required to know how competing prediction systems perform when a set of new samples are to be tested using an already validated model (Shepperd and MacDonell, 2012). To identify the best prediction system, we estimated the percentage relative error deviation (*PRED*) at different threshold levels (T):

$$PRED(T) = \left[\frac{1}{N}\sum_{i=1}^{N}\begin{cases} 1 & if \dfrac{|Y_i - \widehat{Y}_i|}{Y_i} \le T \\ 0 & if \dfrac{|Y_i - \widehat{Y}_i|}{Y_i} > T \end{cases}\right] \times 100 \tag{3}$$

where N is the number of new (unseen) samples (Conte et al., 1986; Shepperd and MacDonell, 2012; Idri et al., 2018; Silhavy et al., 2021). In general, T values range from 25-75 % (Silhavy et al., 2021) and large *PRED* values indicate better estimation accuracy (Idri et al., 2015) for a given model. To estimate optimum T values for our datasets, we calculated *PRED* values at T values of 10, 20, 30, 40, and 50 % for each model. Similarly, the effect of spiking was evaluated based on the RMSE ratio (Ng et al., 2022):

$$RMSEratio = \frac{RMSE_{Spiking}}{RMSE_{Withoutspiking}} \tag{4}$$

and the percentage change in the RMSE values (ΔRMSE) of spiked and unspiked datasets. To make a fair model comparison, we recalculated

Table 2
Mean values for different soil parameters in soil samples collected during 2018 and 2021 from selected districts of the Bundelkhand region. Statistics for basic soil properties and nutrient contents of 2018 are reproduced from Majeed et al. (2023a).

Soil properties	Lalitpur		Jhansi-Babina		Mahoba		Jalaun		Hamirpur		Banda		Chitrakoot		Jhansi-Bamour
Year	2018	2021	2018	2021	2018	2021	2018	2021	2018	2021	2018	2021	2018	2021	2021
No. of samples	176	81	195	60	193	75	109	98	102	51	160	49	177	95	98
Coarse sand, %	51.7	57.1	48.6	**47.5**	18.2	9.46	5.56	2.66	7.92	**8.41**	6.25	5.08	12.1	**11.4**	7.07
Fine sand, %	25.9	18.8	30.9	27.1	38.5	**40.9**	33.3	**38.9**	40.7	**38.8**	42.9	**42.6**	44.8	**45.9**	34.5
Clay, %	9.86	12.9	10.7	**11.1**	19.6	26.5	37.1	**33.8**	19.9	29.9	19.4	27.9	16.7	19.5	33.4
pH	6.66	**6.85**	7.25	7.51	7.59	7.99	8.13	**8.24**	8.29	**8.40**	8.14	**8.10**	7.91	**7.90**	8.19
EC, dS m^{-1}	0.20	0.08	0.23	**0.19**	0.22	**0.21**	0.12	0.19	0.23	**0.26**	0.18	**0.19**	0.14	0.22	0.23
SOC, %	0.66	0.45	0.64	0.57	0.58	0.41	0.32	**0.32**	0.43	0.34	0.51	0.37	0.42	**0.37**	0.40
Av. P	24.4	**27.0**	15.7	32.0	7.88	**6.76**	3.42	9.01	5.47	**5.04**	6.26	**5.09**	8.89	5.09	8.40
Ex. K	76.9	39.6	90.8	**91.5**	167	118	179	**171**	215	**162**	240	166	147	111	137
Ex. Ca	1150	**1046**	1296	1934	3278	**3367**	2799	3437	3723	**3536**	2930	3128	2033	2680	4517
Ex. Mg	206	169	244	**264**	294	354	399	466	454	**487**	416	398	261	307	346
Av. S	10.7	4.41	11.7	**10.2**	17.2	7.67	4.30	6.02	9.80	**9.67**	8.50	**6.50**	5.90	7.88	10.7
Av. Zn	1.21	0.95	0.60	**0.63**	0.42	**0.58**	0.35	0.29	0.35	**0.36**	0.63	0.41	0.61	**0.44**	0.18
Av. B	0.43	0.24	0.41	**0.46**	0.50	**0.43**	0.64	**0.69**	0.84	0.63	0.64	0.48	0.44	0.35	0.56
Av. Fe	20.6	**17.6**	8.13	**10.3**	9.28	6.09	4.77	5.84	3.57	**3.19**	4.84	**4.90**	6.80	7.55	3.35
Av. Cu	0.75	**0.62**	0.70	**0.99**	0.83	**0.81**	0.81	**0.84**	0.63	**0.64**	0.88	**0.80**	0.75	0.90	0.62
Av. Mn	21.7	**18.5**	11.1	**12.8**	10.4	5.54	5.16	**5.07**	6.13	3.22	9.79	5.01	7.47	**7.47**	3.35
Ex. Na	67.3	49.6	64.4	**62.2**	110	**121**	219	**212**	200	**217**	191	117	111	**133**	126

EC: electrical conductivity; SOC: soil organic carbon; Av.: available; Ex.: exchangeable. *All nutrient contents are in mg kg^{-1}. Bold with underlined and bold font cases indicate the Wilcoxon rank sum test at 5% and 10% level of significance, respectively.

RMSE values for all the scenario 1 cases after removing the samples used for spiking from the T_{2021} dataset. We also estimated STCR ratings for each soil parameter in test datasets using their DRS-estimated values. The STCR rating accuracy (SRA) for each soil parameter in a specific test dataset (site-specific, geology-specific, and regional-scale) was then estimated by calculating the percentage of locations for which DRS-estimated and laboratory-measured values of the parameter yielded identical STCR ratings:

$$SRA = \frac{Number\ of\ correctly\ classified\ samples\ in\ the\ DRS\ approach}{Total\ number\ of\ samples} \times 100 \quad (5)$$

3. Results

3.1. Characteristics of soil properties and soil spectra

Table 2 and Table S4 list the mean and the coefficient of variation (CV) values for 17 soil parameters, respectively. Lalitpur and Jhansi-Babina had coarse-textured soil samples with an average sand content > 75 %. Soil samples from Jalaun had the highest average clay content of 37.1 % in 2018 and 33.8 % in 2021 samples. About 78–86 % of Lalitpur and Jhansi-Babina soil samples were sandy loam and loamy sand. Similarly, 66–71 % of Jalaun's soil samples belonged to clay and clay loam textural classes. Thus, both coarse and fine textured soils dominated different sampling sites (development blocks), which may also be seen from the distribution of textural classes in the USDA textural triangles for both 2018 and 2021 samples (Fig. S2). As expected, the SOC content remains low with an average value < 0.66 % across these districts (Table 2). Table S5 shows the descriptive statistics for soil parameters obtained by pooling soil data for the two geology-specific regions of Bundelkhand. The soil samples from the PCG group showed acidic to neutral pH with the first quartile values ranging from 6.79 to 7.17 and third quartile values ranging from 7.68 to 8.10; soil samples from the QSG group showed neutral to alkaline pH with the first quartile values ranging from 7.98 to 8.04 and third quartile values ranging from 8.31 to 8.35. A digital soil map of pH (Fig. S3) created using the T_{2018} dataset shows that the majority of the PCG soils were acidic and QSG were alkaline. The whole study area can be divided into acidic soils of Lalitpur and parts of Jhansi and Mahoba districts in the southwest and alkaline soils in the northeast matching two specific geology of the Bundelkhand region. Matching with soil reaction, PCG soil samples showed higher available soil P concentrations compared to those of QSG soil samples. In contrast, QSG samples showed high exchangeable K, Ca, and Mg concentrations with the third quartile values in the range of 175–242, 3259–4126, and 456–480 mg kg^{-1}, respectively. As for micronutrients, the PCG soil samples showed higher average concentrations for available Zn, Fe, and Mn than QSG soil samples. In turn, QSG soil samples had more available B and exchangeable Na because of prevailing alkalinity. In general, micronutrient contents showed high variability in both the years. Available Zn and Fe showed the highest variance with CV values of 296 % in T_{2018} and 150 % in T_{2021} samples (Table S4). Despite such high variability, the Wilcoxon rank-sum test results (Table 2) showed no significant (p-value < 0.1) difference between T_{2018} and T_{2021} estimates of several parameters (e.g., soil pH, Zn, B, Cu, Fe, Mn, and Na contents) in most districts except for the Jhansi-Babina and Mahoba.

Similar to soil properties, spectral reflectance data also showed diverse characteristics. Typical reflectance spectra for the PCG and QSG soils for T_{2018} (Fig. 3A) and T_{2021} (Fig. 3B) datasets suggest that PCG soils are generally more reflective possibly because of their acidic reaction and resulting high Fe contents (Table S4) than those of QSG soils. Similar results may be seen for the mean reflectance spectra collected for different development blocks during 2018 and 2021 sampling campaigns (Fig. S4) – soils from the Lalitpur and Jhansi-Babina sites are generally more reflective than the remaining sites with Jalaun showing the least reflective soils in our samples. Wan et al. (2019) also observed high reflectance values for acidic soil samples. Results of the principal component analysis on processed soil spectra for both the calibration (T_{2018}) and test (T_{2021}) datasets suggested that the first three PCs of the calibration dataset of PCG, QSG, and regional-scale (all the districts pooled together) could cumulatively explain about 95.7 %, 97.3 %, and 96.2 % of variances, respectively. Resulting biplots using the first 3 PCs along with a convex hull around the calibration data (Islam et al., 2005) in Fig. 3C to Fig. 3E clearly show that some of the T_{2021} data points are outside the calibration space of T_{2018} data although the majority of the test samples were within the spectral space of the calibration datasets. As expected, the regional-scale dataset occupied a larger spectral space with PC1 ranging from −8 to 4 followed by the QSG and PSG datasets. Fig. 3E also captures two distinct patterns in accordance with the distinctive geological origin of the data points.

Table S6 lists the Pearson correlation coefficients (r) among soil chromophores (soil texture, SOC content, and available Fe), soil non-chromophores (pH, EC, and nutrient contents) and PCs of soil spectra.

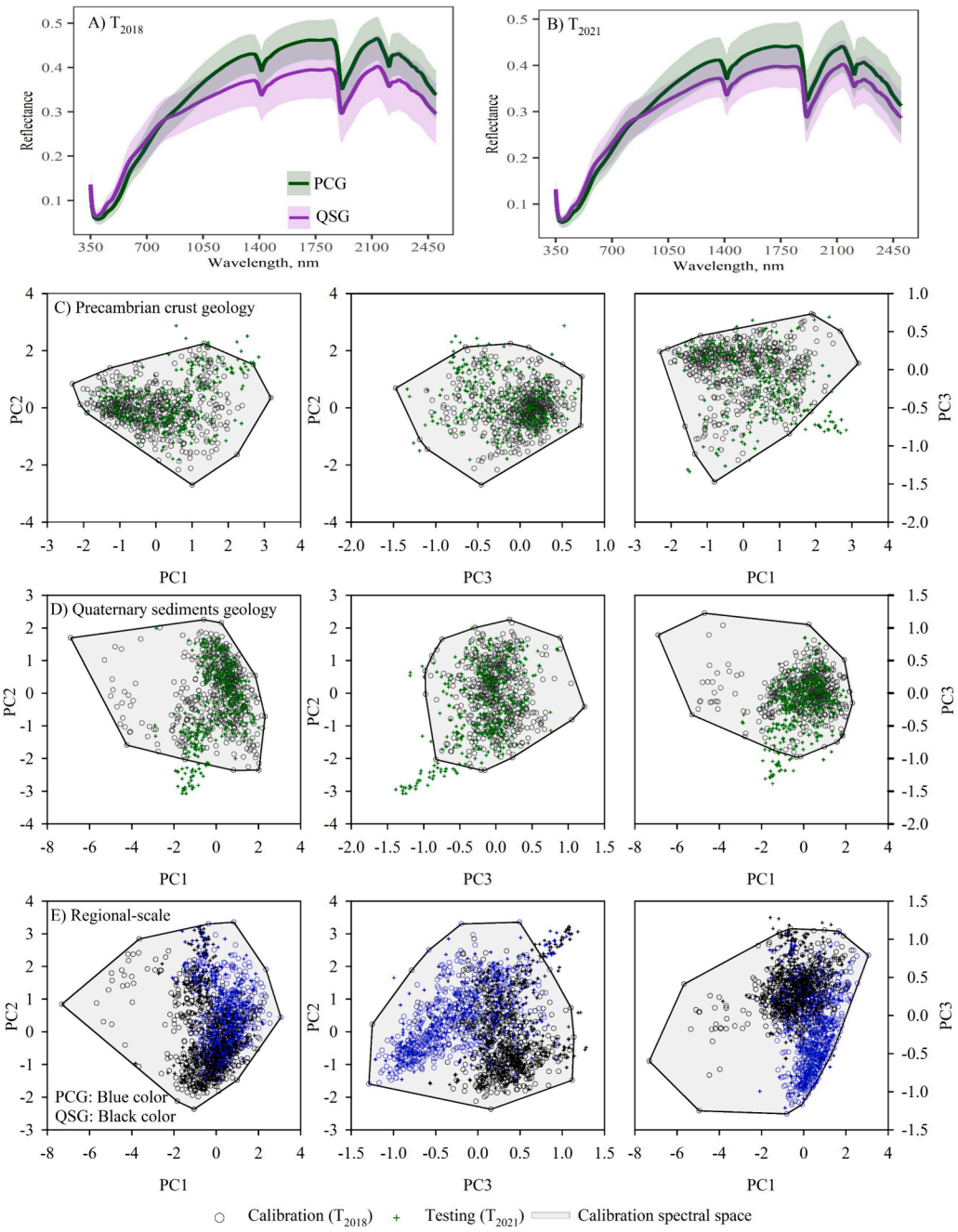

Fig. 3. Average spectral reflectance and their standard deviations of the geology-specific samples collected during 2018 (T2018; A) and 2021 (T2021; B); spectral variability across the Precambrian crust geology (PCG), quaternary sediments geology (QSG), and regional-scale shown in biplots (C, D, and E) using standardized principal components (PC) of pre-processed spectra.

All soil chromophores show a statistically significant (p-value < 0.01) correlation with most of the soil non-chromophores and the PCs of soil spectra. For instance, clay contents showed moderate negative correlation with available P, Zn and Mn in both years and moderate to strong positive correlation with remaining nutrients (r: 0.20 to 0.82). Soil pH showed strong negative correlation with coarse sand and available Fe contents (r: −0.55 to −0.66). Available soil P had a strong positive correlation with coarse sand (r: 0.51 to 0.68) and moderate positive correlation with the SOC (r: 0.53 to 0.36). Exchangeable K has a moderate negative correlation with coarse sand and exchangeable Ca and Mg have a strong negative correlation with coarse sand (r: −0.51 to −0.69). Most available micronutrients showed moderate positive correlation with SOC content whereas available Cu and Mn were positively correlated with available Fe (r: 0.41 to 0.62). Interestingly, both EC and available S showed no linkage with any of the soil chromophores making them least probable to be estimated in the DRS approach for our study sites. Sarathjith et al. (2016) have shown that the effectiveness of the DRS approach to estimate a soil non-chromophore strongly depends on its linear and non-linear dependencies on multiple soil chromophores. Thus, the DRS approach is expected to perform well for most of our soil parameters except for EC and available S.

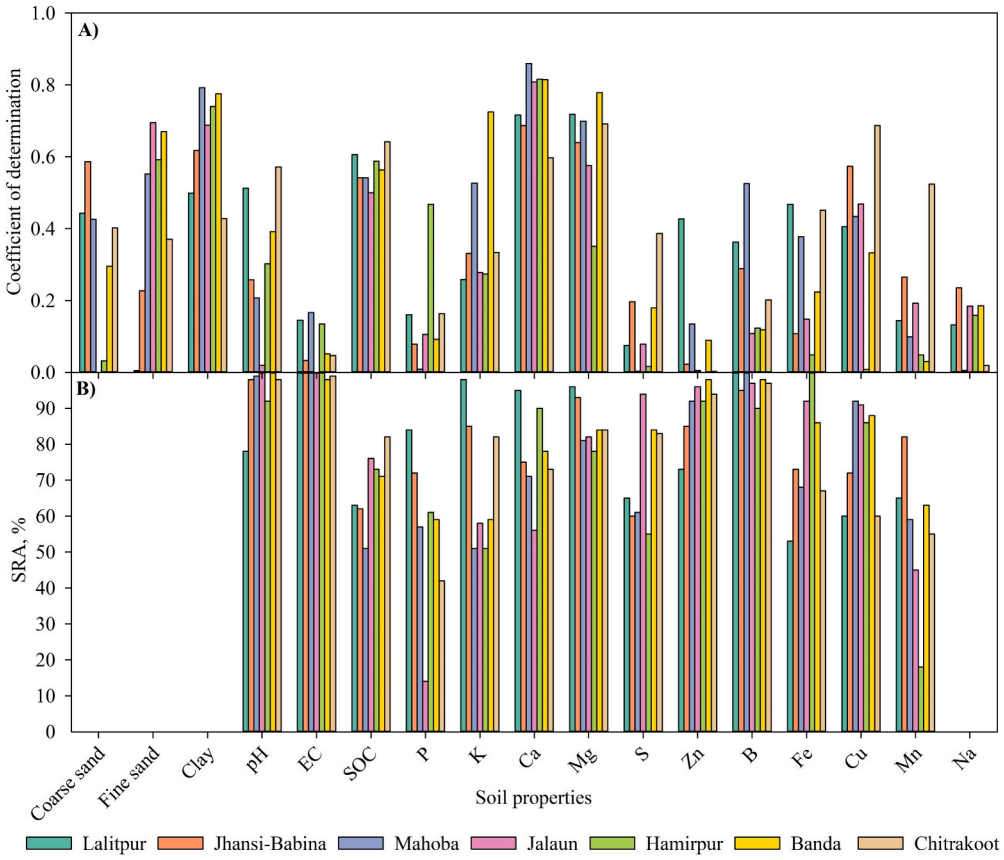

Fig. 4. Performance evaluation of reflectance spectroscopy approach in scenario 1 (test samples collected from within the calibration zone) for site-specific testing; bar plots show the coefficient of determination (A) and STCR rating accuracy (SRA; B) values for 17 soil parameters.

3.2. Performance of chemometric models under selected modeling scenarios

3.2.1. Scenario 1: Test samples from within the calibration zone

Fig. 4 shows that R^2 and SRA values obtained for the site-specific T_{2021} datasets using the cross-validated Cubist model in respective T_{2018} datasets; resulting RMSE and bias values are listed in Table S7. Out of 119 test cases (17 parameters x 7 development blocks), only 22 test cases show $R^2 > 0.6$. Specifically, exchangeable Ca and clay contents were the best estimated soil parameters in each development block with R^2 values ranging from 0.60 (Chitrakoot) to 0.82 (Hamirpur) and from 0.43 (Chitrakoot) to 0.79 (Mahoba), respectively. Similarly, exchangeable Mg also showed consistent performance in all the sites with R^2 values ranging from 0.58 (Jalaun) to 0.78 (Banda), except for the Hamirpur. The SOC content was the next best predicted parameter with moderate performance in different development blocks (R^2: 0.50–0.64;

Table 3
Performance of the diffuse reflectance spectroscopy approach for scenario 1 where test samples were collected from within the calibration zone and tested on geology-specific and regional-scale datasets.

Soil properties	Geology-specific testing								Regional-scale testing			
	Precambrian crust				Quaternary sediments							
	R^2	RMSE	Bias	SRA	R^2	RMSE	Bias	SRA	R^2	RMSE	Bias	SRA
Coarse sand, %	0.89	8.91	−1.82	NA	0.65	3.85	−0.58	NA	0.92	6.30	−1.05	NA
Fine sand, %	0.68	8.27	1.03	NA	0.65	7.40	0.41	NA	0.70	7.75	0.38	NA
Clay, %	0.82	5.11	−1.37	NA	0.78	6.09	−3.87	NA	0.82	5.60	−2.67	NA
pH	0.77	0.38	−0.17	93	0.42	0.29	0.06	98	0.75	0.32	−0.04	96
EC, dS m^{-1}	0.14	0.12	0.01	100	0.05	0.13	−0.06	99	0.08	0.13	0.00	100
SOC, %	0.56	0.18	0.10	57	0.49	0.11	0.01	75	0.57	0.14	0.06	70
Av. P	0.47	15.3	−8.06	62	0.02	6.21	−0.54	44	0.59	10.5	−4.52	54
Ex. K	0.59	61.1	32.6	77	0.40	84.1	34.6	58	0.52	70.8	28.0	68
Ex. Ca	0.91	688	294	85	0.80	662	−467	73	0.88	510	−80.2	85
Ex. Mg	0.68	77.4	−4.10	90	0.71	87.4	5.9	85	0.76	77.7	−2.30	88
Av. S	0.12	6.66	1.34	69	0.02	8.06	−1.30	74	0.04	7.78	−0.16	67
Av. Zn	0.21	0.62	−0.11	86	0.04	0.35	0.04	97	0.37	0.41	−0.04	93
Av. B	0.40	0.19	0.03	97	0.04	0.56	0.22	84	0.52	0.18	0.03	97
Av. Fe	0.50	9.60	2.12	65	0.51	2.81	−1.31	89	0.49	6.77	1.02	83
Av. Cu	0.37	0.40	0.10	72	0.42	0.25	−0.08	81	0.38	0.31	0.00	82
Av. Mn	0.56	6.02	1.28	60	0.37	2.60	0.18	61	0.53	5.02	1.27	55
Ex. Na	0.06	96.0	6.80	NA	0.23	117	25.2	NA	0.33	101	14.3	NA

R^2: coefficient of determination; RMSE: root-mean-squared error; SRA (%): STCR rating accuracy; EC: electrical conductivity; SOC: soil organic carbon; Av.: available; Ex.: exchangeable; NA: not applicable. All nutrient contents are in mg kg^{-1}.

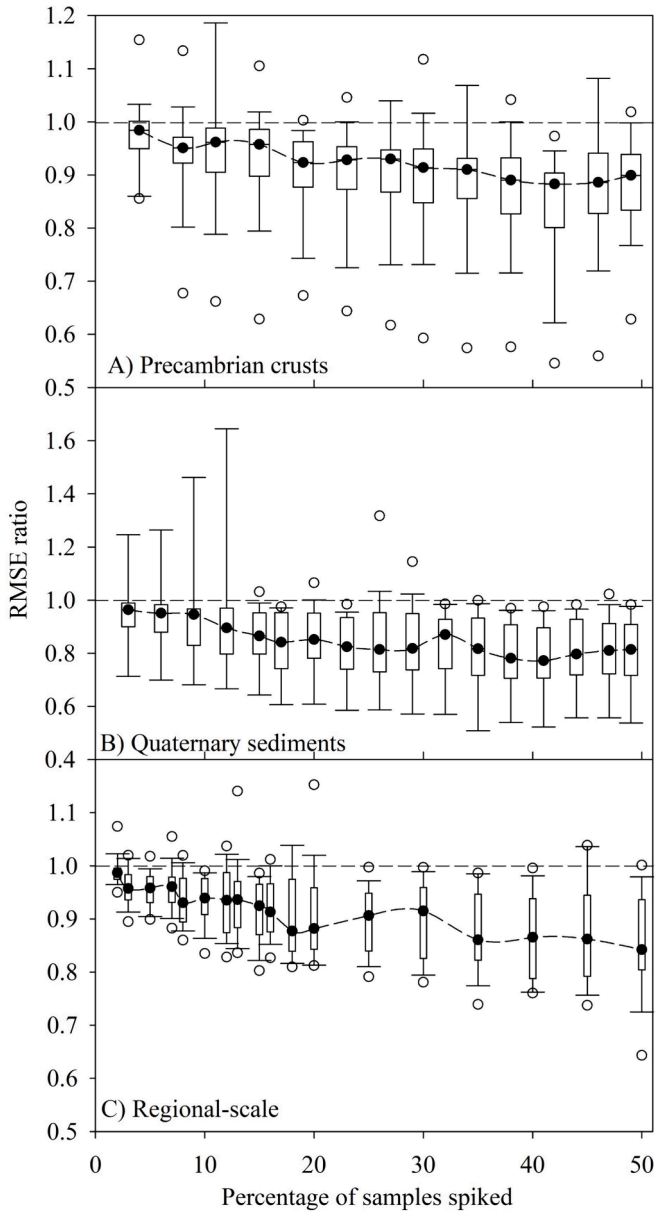

Fig. 5. Boxplots of root-mean-squared error (RMSE) ratio for the spiking approach tested on geology-specific (A and B) and regional-scale (C) datasets at various percentage of samples spiked. The median values are shown with filled black circles connected with dashed line.

RMSE: 0.08 to 0.22 %). Except for these four soil parameters, no other soil parameters could not be estimated with reasonable accuracy. In contrast, the results of the estimated STCR values suggested close match between the DRS-based and conventional soil test ratings even in site-specific test datasets.

With the SRA values in the range of 14 to 100 % for T_{2021} datasets, 13 out of 17 parameters (63 out of 119 test cases) showed identical STCR ratings in more than 70 % samples. Such a close match between these two methods of soil testing in test datasets suggest that temporal applicability at the individual development block level is possible for STCR ratings in the DRS approach. Because the coordinates of T_{2018} samples are different from those of T_{2021} samples, the temporal applicability of trained models for STCR ratings are indeed spatio-temporal in nature. Thus, if the management goal is to make nutrient recommendation alone, one could safely use DRS approach for soil testing.

The performance statistics for the Cubist model in geology-specific and regional-scale datasets are listed in Table 3. Out of 17 soil properties, five soil properties (three textural fractions, exchangeable Ca, and Mg) were well estimated in all three broad spatial scales (PCG, QSG, and regional-scale) with $R^2 > 0.6$ (Table 3). Soil pH was the next well-estimated soil property with R^2 values ranging from 0.42 (QSG) to 0.77 (PCG). Similar to site-specific testing, SOC content showed moderate performance with R^2 and RMSE values ranging from 0.49 to 0.57 and from 0.11 to 0.18 %, respectively. Available Fe and exchangeable K also showed moderate performance in all three spatial scales with R^2 values ranging from 0.49 to 0.51 and from 0.40 to 0.59, respectively. Soil properties such as available P, B, and Mn were moderately estimated with $R^2 > 0.40$ in PCG and regional-scale datasets; QSG samples showed slightly poor performance than their PCG and regional counterparts. Available Cu was better estimated in QSG than PCG and regional-scale datasets. Overall, most of the soil properties in PCG region were better estimated than the QSG region (Table 3). As expected, the EC and available S could not be estimated in the DRS approach possibly because of their weak correlation with different soil chromophores.

Results of the STCR-based nutrient recommendations for the broad soil groups suggested that the SRA values are in the range of 44 to 100 % for T_{2021} dataset with 27 out of 39 test cases (13 out of 17 parameters) showing similar STCR ratings in more than 70 % samples. These results suggested that the DRS models calibrated using both the geology-specific and regional-scale datasets performed better than those of site-specific models. Compared to site-specific dataset both the geology-specific and regional-scale datasets had greater variability in these pooled datasets, which may have contributed to better performance of the Cubist model in their test data.

3.2.2. *Scenario 2: Spiking approach*

Fig. 5 shows RMSE ratios at different percentages of spiked samples for both the geology-specific and regional-scale datasets; corresponding site-specific boxplots are shown in Fig. S5. Although there is no clear threshold for the percentage of samples to be spiked (no global minima), the RMSE ratios shows a clear decreasing trend with the increase in the number of spiking samples in the calibration datasets. For the site-specific datasets, the very first local minimum for the median RMSE ratio appeared when 15 to 25 percentage of samples were selected for spiking calibration data (Fig. S5) although the improvement because of site-specific spiking is not that significant. In contrast, Fig. 5 shows several local minima for geology-specific and regional-scale datasets, with 20 % spiking being particularly notable with RMSE ratio < 1. From cost considerations, a 20 % spiking threshold was earlier recommended by Luce et al. (2022). Overall, while site-specific spiking shows limited benefits, a 20 % spiking threshold may be an effective choice for threshold in cases of large-scale datasets such as those of geology-specific and regional-scale data.

Performance statistics resulting from spiking geology-specific and regional-scale datasets using 20 % of T_{2021} data are listed in Table S8. We used the RMSE ratio, percentage decrease in RMSE (ΔRMSE), and percentage increase in SRA (ΔSRA) values (Table 4) for evaluating the effects of spiking. Both Table S8 and Table 4 clearly show that spiking T_{2018} data with the 20 % of cLHS-selected T_{2021} datasets outperformed the modelling cases under scenario 1 (no spiking condition) for most soil parameters in both geology-specific and regional-scale datasets. Out of 17 soil parameters, 9 parameters of the PCG, 7 parameters of the QSG, and 9 parameters of the regional-scale datasets were well-estimated with $R^2 > 0.6$ (Table S8). Notably, spiking approach improved the macro- and micro-nutrient estimation in the geology-specific dataset especially for the QSG region. Possible reason may be in the spiking approach majority of the soil samples lied within the calibration spectral space (Fig. 6B) than those without spiking approach (Fig. 3D). In addition to five soil parameters that showed good performance in scenario 1, spiking improved the estimation of other soil properties such as SOC content, available P, Zn, Fe, Cu, exchangeable K, and Na with ΔRMSE values in the ranges of 12–22 %, 7–22 %, 4–15 %, 8–19 %, 16–26 %, 15–26 %, and 4–5 %, respectively (Table 4). Available B in QSG dataset showed the

Table 4
The effect of spiking in geology-specific and regional-scale datasets.

Soil properties	RMSE ratio			ΔRMSE			ΔSRA		
	PCG	QSG	RS	PCG	QSG	RS	PCG	QSG	RS
Coarse sand, %	0.95	0.98	0.94	5	2	6	NA	NA	NA
Fine sand, %	0.97	0.96	0.93	3	4	7	NA	NA	NA
Clay, %	0.92	0.80	0.85	8	20	15	NA	NA	NA
pH	0.91	0.99	0.94	9	1	6	1	–	1
EC, dS m^{-1}	0.98	0.93	0.83	2	7	17	–	–	–
SOC, %	0.86	0.78	0.88	14	22	12	8	6	2
Av. P	0.93	0.78	0.84	7	22	16	6	19	16
Ex. K	0.82	0.74	0.85	18	26	15	6	13	5
Ex. Ca	0.67	0.68	0.84	33	32	16	1	14	3
Ex. Mg	0.89	0.86	0.87	11	14	13	1	1	–
Av. S	1.00	0.94	1.02	0	6	–	3	2	4
Av. Zn	0.92	0.85	0.96	8	15	4	–	1	1
Av. B	0.98	0.34	1.12	2	66	–	–	13	–
Av. Fe	0.92	0.81	0.82	8	19	18	9	3	2
Av. Cu	0.76	0.84	0.74	24	16	26	10	4	3
Av. Mn	0.96	1.07	0.81	4	–	19	6	5	8
Ex. Na	0.96	0.95	0.95	4	5	5	NA	NA	NA

PCG: Precambrian crusts geology; QSG: Quaternary sediments geology; RS: regional-scale; RMSE: root-mean-squared error; ΔRMSE: percentage decrease in RMSE; ΔSRA: incremental change in STCR rating accuracy percentage; EC: electrical conductivity; SOC: soil organic carbon; Av.: available; Ex.: exchangeable; NA: not applicable. All nutrient contents are in mg kg^{-1}. The dash symbol represents that the property did not show any improvement in modelling over the compared modelling scenario.

highest improvement with a R^2 value changing from 0.04 without spiking (Table 3) to 0.51 with spiking (Table S8); resulting ΔRMSE value was as high as 66 %. Spiking approach also showed high STCR classification accuracies with 10 out of 13 parameters of PCG, 11 out of 13 parameters of QSG, and 12 out of 13 parameters of regional-scale datasets showing similar STCR ratings in more than 70 % samples (Table S8). However, EC, available S, and exchangeable Na remained as the least probable candidate to be estimated by the DRS approach (Table S8 and 4). Fig. 7 shows observed versus predicted cases for some of the selected soil parameters such as exchangeable Ca, SOC contents, available B, and S for the scenario 1 and 2. Among all the parameters, exchangeable Ca showed the best prediction for spiking scenario (Fig. 7). A slight improvement for the spiking approach in the case of SOC may also be seen in Fig. 7. The scatterplot for available B shows that a few soil samples from QSG region without spiking were overestimated reducing the accuracy, which improved through spiking (Fig. 7C). Widely-scattered data along 1:1 line in Fig. 7 shows the extent of error in the predicted data for the poorly-predicted available S in our geology-specific dataset. This may be because of the weak correlation of between S with known soil chromophores (Table S6).

3.2.3. Scenario 3: Localizing approach

Fig. 8 shows the boxplots of the RMSE ratio obtained using the geology-specific and regional-scale Cubist models developed in scenarios 1 and 2 and tested individually on each site-specific T_{2021} datasets (7 development blocks). Spiking the T_{2018} calibration data with 20 % of T_{2021} data (temporal spiking) in the case of both the geology-specific and regional-scale datasets improved the model performance (lower RMSE ratio) compared to the site-specific models of scenario 1 suggesting effective localization of broader datasets. However, there is no consistent trend among these three broad-scale models supporting a specific model consistently outperforming the other across all development sites. For instance, spiking regional-scale datasets showed improved performance in 4 out of 7 development blocks with their third quartile RMSE ratio values < 1 and with low median values (Fig. 8). Spiking geology-specific datasets performed better when the resulting models were localized to Lalitpur, Jhansi-Babina, and Hamirpur sites compared to their respective regional-scale models.

Table 5 shows the improvement in the RMSE and SRA values obtained by localizing the best performing Cubist models in estimating soil properties at each development block over their site-specific models obtained in scenario 1. Out of 119 test cases (17 parameters x 7 sites), 102 cases show reduction in error while localized with a spiked dataset compared to site-specific testing under scenario 1 (no spiking scenario) with ΔRMSE values ranging from 1 % to 89 %. Soil properties such as exchangeable Mg, available P, B, Mn, clay, and fine and coarse sand contents showed decreased error percentage in all development blocks with ΔRMSE values in the ranges of 10–51 %, 1–86 %, 8–70 %, 3–88 %, 8–37 %, 2–22 %, and 2–54 %, respectively. Estimation errors for micronutrients also decreased for the development blocks such as Jalaun, Hamirpur, Banda, and Chitrakoot with ΔRMSE values ranging from 3 % to 88 %. Specifically, most soil parameters showed decrease in the estimation error at Hamirpur site followed by Jalaun and Banda (Table 5). Similarly, 52 out of 91 test cases show an increase in the number of samples having similar STCR ratings for both DRS- and wet chemistry-based approaches with increments ranging from 2 to 48 % (Table 5). The SRA values for exchangeable Ca increased in all the development blocks with a range from 2 to 26 %. Macro-nutrients such as available P and exchangeable K also showed improvement in the SRA values with a range of 2–48 % and 3–34 %, respectively. Similar to ΔRMSE values, most of the soil properties in Hamirpur district showed an incremental change in the SRA values. Scenario 1 is a case of only temporal transferability. When broader-scale datasets (geology-specific and regional-scale) were spiked with data from T_{2021} under scenario 3, the applicability of the trained DRS models yielded better model performance suggesting that localizing and spiking together may be advocated for soil testing in new samples.

3.2.4. Scenario 4: Applicability of calibrated models to spatially- and temporally-independent dataset

Soil samples collected at the Jhansi-Bamour development block served as a spatially- and temporally-independent dataset in our study. Fig. 9 shows resulting R^2 and SRA values obtained using cross-validated Cubist models from our three broad datasets (two geology-specific and one regional-scale) with and without spiking. Resulting RMSE and bias values are listed in Table S9. As seen in scenario 3 (localizing approach), models using spiked geology-specific and regional-scale datasets performed better than those without spiking; regional-scale datasets generally outperformed all other modelling approaches in estimating most of the soil properties of Jhansi-Bamour site (Table S9). Specifically, soil textural fractions of clay and fine sand contents and exchangeable Ca and Mg were well-estimated using the spiked regional-scale dataset with R^2 values ranging from 0.71 to 0.91 (Fig. 9). As in the case of scenario 1, SOC content was the next best predicted parameter with R^2

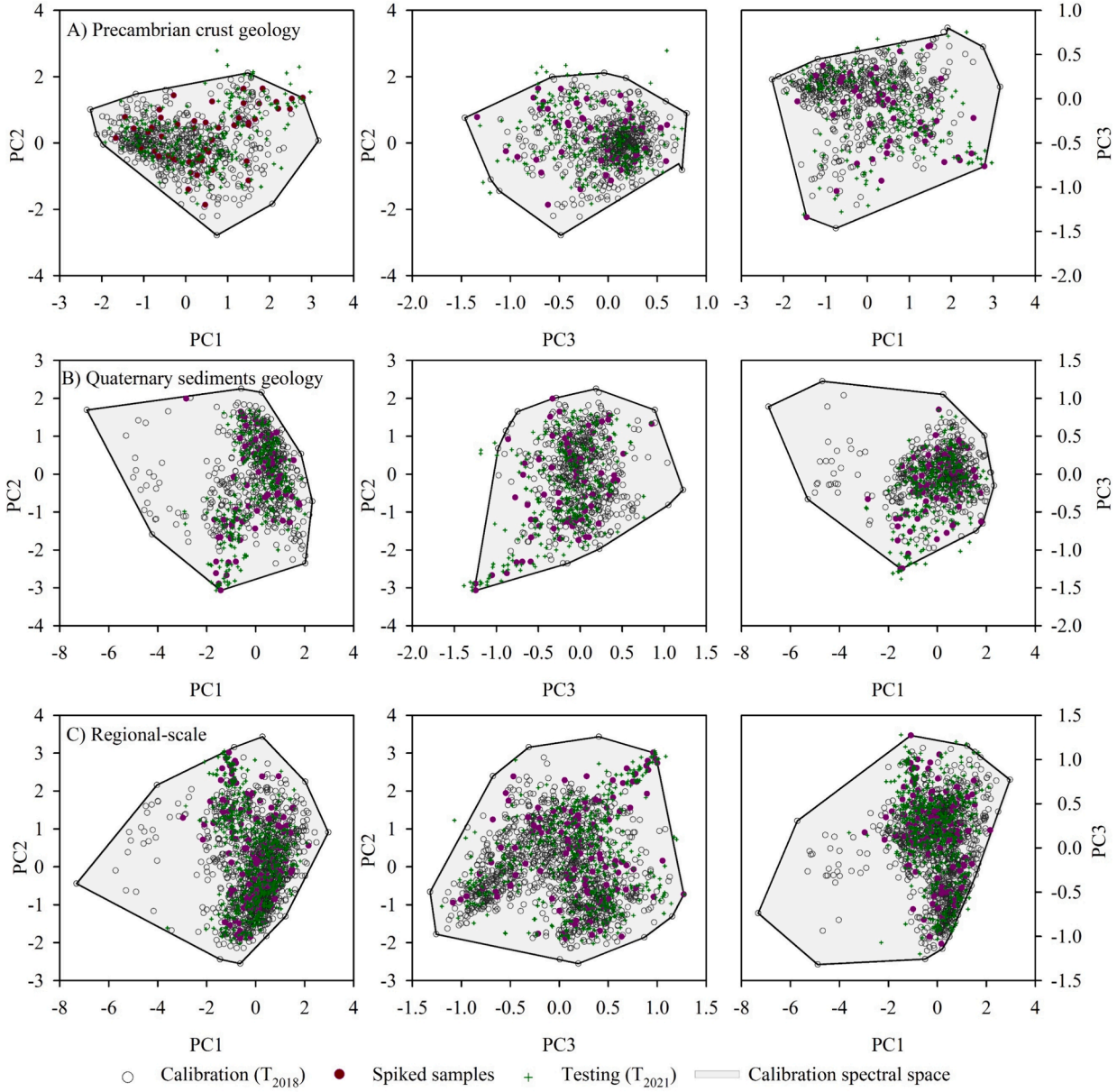

Fig. 6. Convex hull biplots for the Precambrian crust geology (PCG), quaternary sediments geology (QSG), and regional-scale shown in plots (A, B, and C) using standardized principal components (PC) in the scenario 2 (spiking approach).

and RMSE values of 0.60 (Fig. 9) and 0.10 % (Table S9), respectively (moderate performance). Available B also showed moderate performance with R^2 value of 0.59. Interestingly, there are improvements in the estimation of soil properties such as EC, available P, S, Zn, and exchangeable Na compared to other site-specific test cases of scenario 1. However, parameters such as available Fe and coarse sand in Jhansi-Bamour samples could not reasonably be estimated using any of the modelling scenarios. For the STCR ratings, reasonable classification accuracies were seen in the range from 47 % to 100 %, with 10 out of 13 soil parameters showing > 70 % SRA values (Fig. 9). The Jhansi-Bamour site represents a true test site with no spatial and temporal overlap between training and test datasets. With the spiked regional-scale models, several soil parameters in Jhansi-Bamour showed strong classification accuracies suggesting acceptable spatio-temporal applicability of trained DRS models for the case of STCR ratings.

3.3. Estimation efficiency of chemometric models in new samples

The best-performing modelling approaches and their general performance for different development blocks, geology-specific region, and the whole region (Bundelkhand) are listed in Table S10. As expected, not all the parameters are estimable with the DRS approach to match soil test results from conventional wet chemistry-based methods. Therefore, we estimated the *PRED* values at varying error thresholds for each of these modelling cases to identify how many samples from our sampling campaign could be tested with a preassigned error threshold. Fig. 10 shows boxplots for estimated *PRED* values of 17 different soil parameters at selected threshold (*T*) values for each development block at a finer scale and two broader scales of having similar geology and the whole study site representing Bundelkhand-specific spectral model. Increasing *PRED* values with the threshold levels suggest that the percentage of samples that can be tested accurately decreases as we increase error threshold. Fig. 10 also shows that the median *PRED*(30) values exceed 60 % for almost all datasets except for the Lalitpur, Jhansi-Babina, PCG,

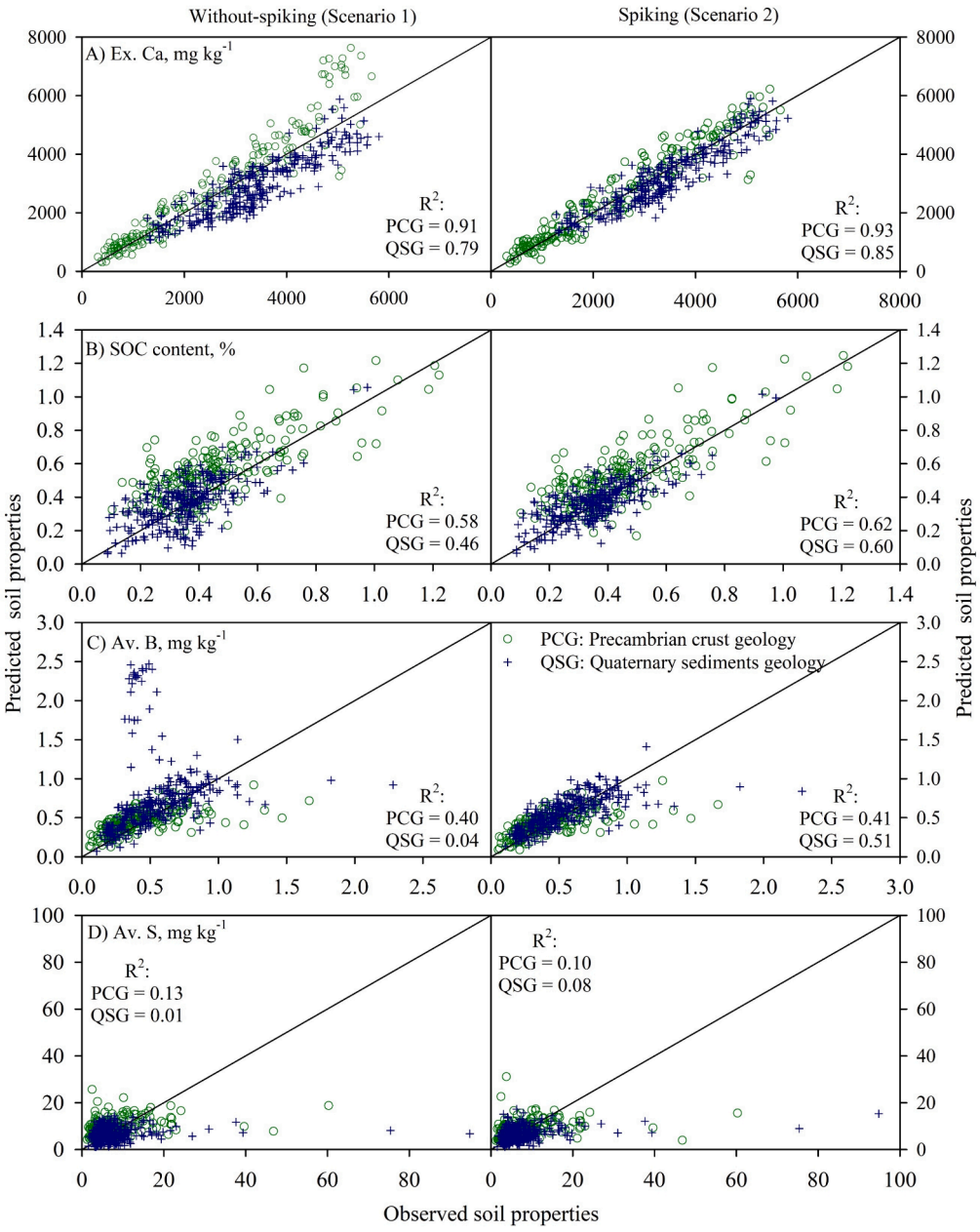

Fig. 7. Scatter plots showing observed vs. predicted values of selected soil properties for no spiking (scenario 1) and spiking (scenario 2) modelling approaches tested on geology-specific test dataset.

and regional-scale datasets. Thus, we may generalize that about 60 % of all new samples can be estimated with an error tolerance of 30 % (i.e., accuracy of > 70 %) for most soil properties. In fact, 59 out of 119 model cases in all development blocks showed > 60 % of samples having < 30 % error. Similar results were found for Jhansi-Bamour soil samples when the regional-scale spiked models were used to test this dataset (Fig. 10).

Fig. 11 shows scatterplots for selected soil properties to critically examine the effectiveness of *PRED*(30) in assessing the estimation efficiency of the DRS. Exchangeable Ca in Jhansi-Bamour showed excellent predictability in test samples (R^2 = 0.91) with estimates closely distributed along 1:1 line of the scatterplot. Exchangeable Ca in Jhansi-Bamour showed *PRED*(30) value of 100 % suggesting that 100 % of the soil samples from this independent test site were estimated with < 30 % error (Fig. 11A). In contrast, the fine sand in Lalitpur had an R^2 value of 0.18 and a *PRED*(30) value of 32 % (Fig. 11B), clearly showing that fine sand was poorly estimated based on both the metrics. Fig. 11A and 11B show that the *PRED*(30) values provide similar inference as R^2 values. However, available Fe in Jhansi-Babina had R^2 value of 0.68 in the test dataset. Yet, Fig. 11C shows that available Fe in most of the soil samples of Jhansi-Babina site are overestimated, which was correctly captured by the *PRED*(30) with a value of 23 %. Similarly, only 8 to 10 data points for available P in Mahoba are widely scattered around 1:1 line resulting in R^2 value of just 0.12 and showed high *PRED*(30) value of 51 % indicating many of the samples can be accurately estimated (Fig. 11D). These results suggest that *PRED*(30) may be used as an additional metric for evaluating the efficiency of the prediction approach in addition to the standard metrics such as R^2 and RMSE among others. We further observed that *PRED* may also have limitations specifically when a soil parameter has inherently less variability such as the case of most soil pH measurements. In our datasets, soil pH had low variability and showed 100 % *PRED*(30) values in PCG and Jhansi-Bamour. Interestingly, soil pH showed R^2 value of 0.79 in PCG samples and just 0.21 in Jhansi-Bamour samples (Fig. 11E and F). Except for pH, most of our soil properties had a wide range and high variability (Table S4) allowing the

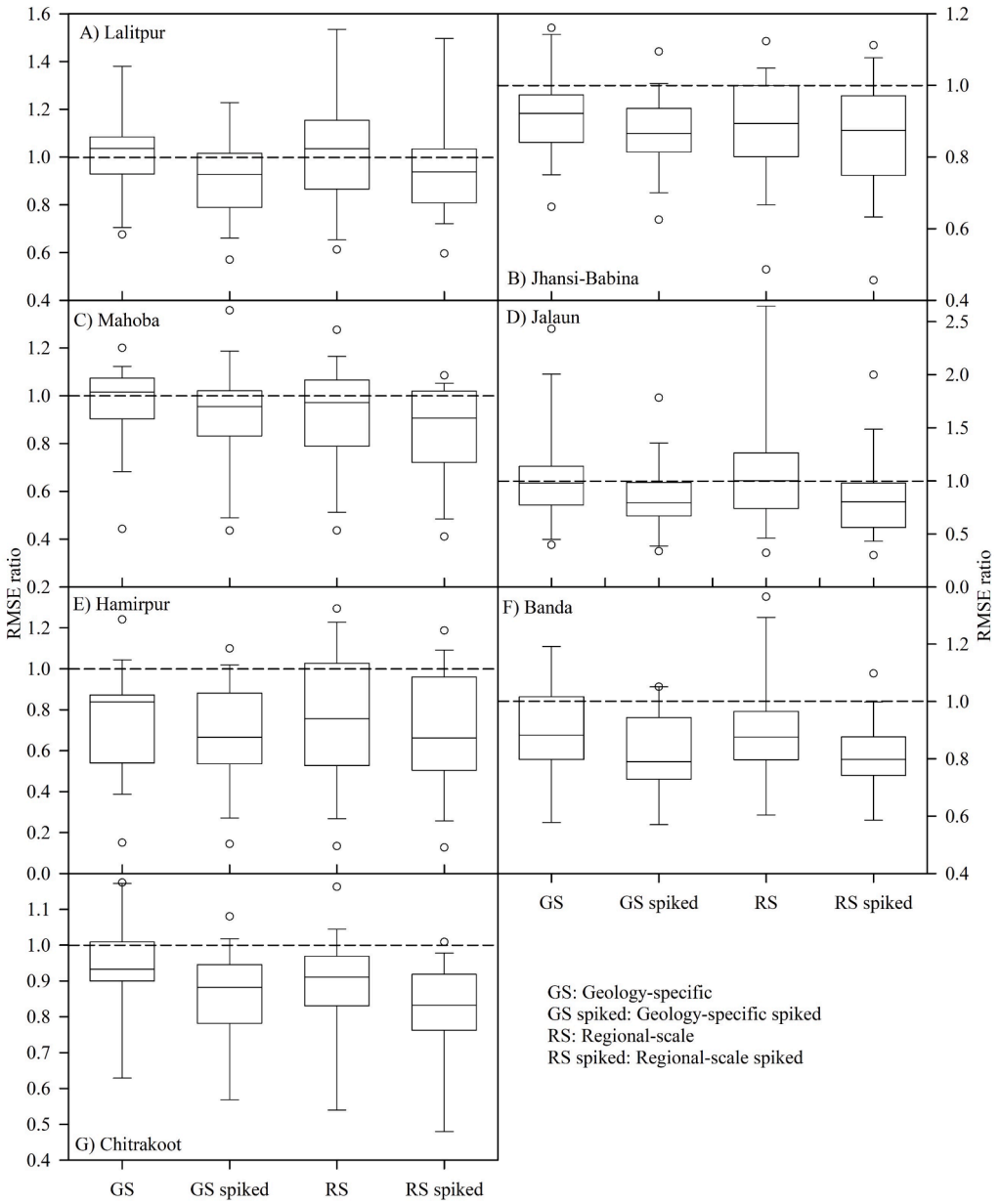

Fig. 8. Boxplots for root-mean-squared error (RMSE) ratio in scenario 3, where the geology-specific and regional-scale models in without-spiking and spiking scenarios were localized to site-specific testing.

use of *PRED* as an efficient metric for estimating soil parameters in test samples.

The *PRED*(30) values for 17 soil properties obtained using the best modeling approaches for each development block, geology-specific, and regional-scale datasets are listed in Table 6. Exchangeable Ca and Mg were well estimated with *PRED*(30) values > 75 % in all datasets except for the Lalitpur district (Table 6). Clay and fine sand contents were also well estimated with *PRED*(30) values ranging from 75 % to 95 % and 76 % to 98 %, respectively. In regions with dominantly coarse textured soils (e.g., Lalitpur and Jhansi-Babina), coarse sand was well estimated with *PRED*(30) values > 75 %. Similarly, SOC content showed moderate to good estimation accuracy across the datasets with *PRED*(30) values ranging from 52 % to 86 % (Table 6). Micronutrients such as available B, Cu, and Fe were moderate- to well-estimated in different development blocks with *PRED*(30) values ranging from 35-88 %, 23–78 %, and 40–92 %, respectively. Soil properties such as EC, available S, Zn and exchangeable Na showed poor estimation accuracy across development blocks and a moderate estimation accuracy in geology-specific and regional-scale datasets. Regions with predominantly coarse-textured soils showed poorer estimation accuracy for most soil properties compared to regions with clay and clay loam textures. In the independent test dataset, 8 out of 17 soil properties showed *PRED*(30) values > 75 %, which is an encouraging result for the DRS approach. For geology-specific datasets, the QSG datasets were better estimated than the PCG datasets for most soil properties. This may be because spiking expanded the spectral space of the calibration data in QSG dataset reducing the number of outliers (Fig. 6). In contrast, in the PCG dataset, most spiking samples selected by the cLHS approach were within the calibration spectral space and could not capture the diverse spectral features of samples outside this space. Overall, the modeling approaches showed good performance in estimating several soil properties, particularly in regions with finer textures. The QSG dataset provided better estimation accuracies than the PCG dataset, highlighting the importance of selecting diverse spiking samples for calibration.

Table 5
The effect of localizing approach in site-specific estimation of soil properties.

Soil properties	Lalitpur		Jhansi-Babina		Mahoba		Jalaun		Hamirpur		Banda		Chitrakoot	
	ΔRMSE	ΔSRA	ΔRMSE	ΔSRA	ΔRMSE	ΔSRA	ΔRMSE	ΔSRA	ΔRMSE	ΔSRA	ΔRMSE	ΔSRA	ΔRMSE	ΔSRA
CS	2	NA	7	NA	9	NA	54	NA	41	NA	27	NA	6	NA
FS	7	NA	2	NA	6	NA	2	NA	22	NA	21	NA	3	NA
Clay	32	NA	15	NA	8	NA	18	NA	37	NA	29	NA	17	NA
pH	8	8	15	3	16	–	19	–	–	–	23	–	–	–
EC	–	–	6	–	–	–	23	–	–	–	3	–	21	–
SOC	7	9	13	–	24	18	–	–	39	6	19	21	13	2
Av. P	2	2	13	13	1	10	46	48	86	16	15	–	24	25
Ex. K	21	4	24	–	59	34	–	–	32	3	14	15	4	–
Ex. Ca	–	2	28	3	31	6	70	26	53	13	–	6	35	14
Ex. Mg	21	2	20	–	24	12	43	–	51	10	10	6	13	4
Av. S	–	15	17	3	39	4	–	–	22	6	8	–	10	2
Av. Zn	–	2	5	–	–	–	20	–	33	6	20	–	88	4
Av. B	24	–	8	–	12	–	38	–	70	10	24	3	21	–
Av. Fe	8	6	37	–	–	16	44	2	10	–	17	6	43	18
Av. Cu	43	6	15	3	–	–	12	–	14	–	24	15	23	18
Av. Mn	20	–	7	–	50	6	3	–	34	19	88	3	22	5
Ex. Na	2	NA	–	NA	–	NA	21	NA	1	NA	30	NA	12	NA

RMSE: root-mean-squared error; ΔRMSE: percentage decrease in RMSE; ΔSRA: incremental change in STCR rating accuracy percentage; CS: coarse sand; FS: fine sand; EC, dS m^{-1}: electrical conductivity; SOC, %: soil organic carbon; Av.: available; Ex.: exchangeable; NA: not applicable. All nutrient contents are in mg kg^{-1} and textural parameters are in %. The dash symbol represents that the property did not show any improvement in modelling over the compared modelling scenario.

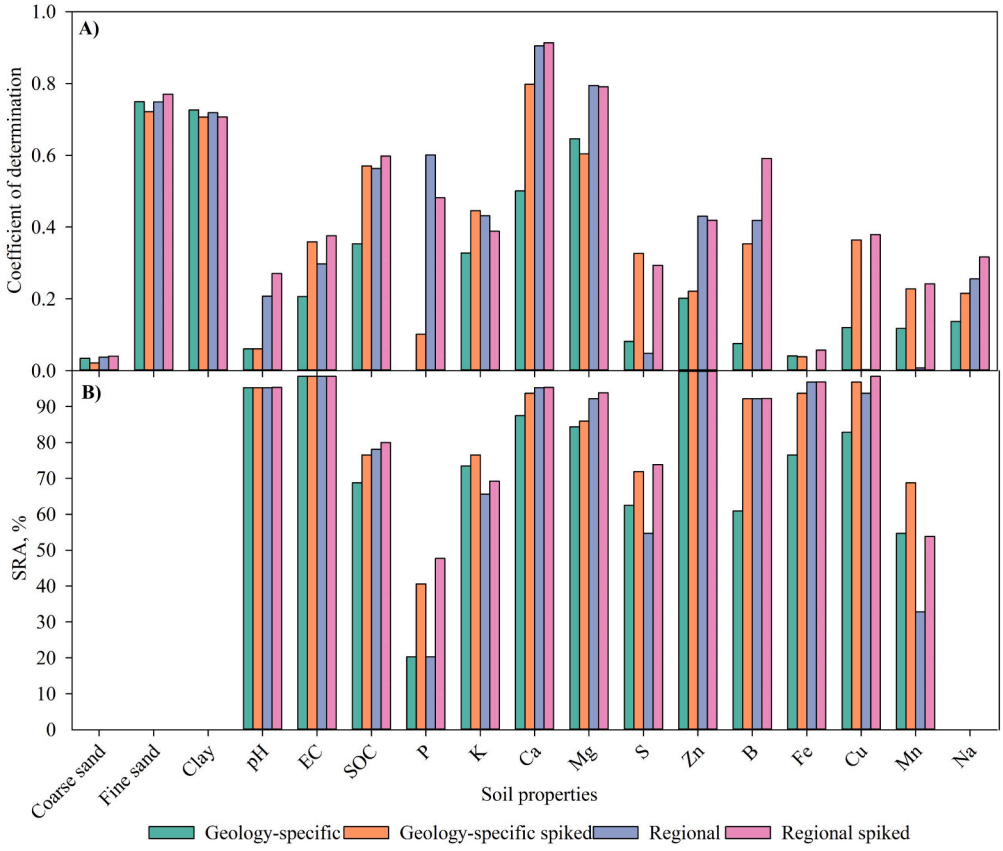

Fig. 9. Performance evaluation of reflectance spectroscopy approach in scenario 4 (Model applicability of calibrated models to spatially- and temporally-independent dataset): test samples are collected from Jhansi-Bamour; bar plots show the coefficient of determination (A) and STCR rating accuracy (SRA; B) values for 17 soil parameters.

4. Discussion

Several studies have examined various aspects of DRS model applicability. Specifically, applicability of trained models across different study areas (Sudduth and Hummel, 1996; Minasny et al., 2009; Grunwald et al., 2018; Zhao et al., 2022), different land use types (Liu et al., 2014; Wang et al., 2014), and between geographic scales such as those calibrated at a global or regional scale and applied to local scales (Shepherd and Walsh, 2002; Brown, 2007; Guerrero et al., 2010; Sanderman et al., 2020; Ng et al., 2022) have been reported. Interestingly, only four recent studies focus on temporal aspects of model applicability (Table 1), possibly because of the challenge associated with repeating sampling campaigns to create both spatially- and temporally-independent test datasets. Also, distinguishing uncertainties in

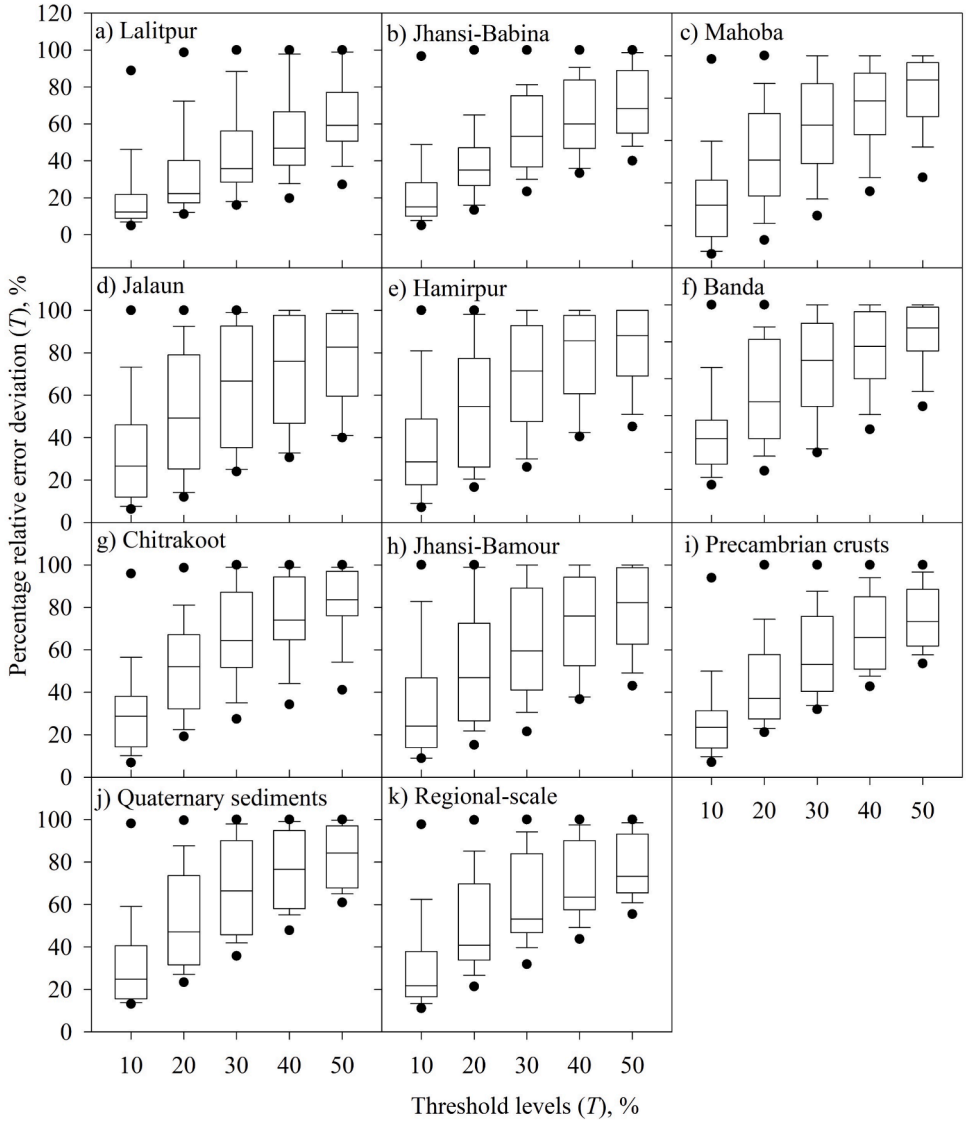

Fig. 10. Boxplots for percentage relative error deviation at different threshold levels (*T*) for site-specific, geology-specific, and regional-scale datasets (all 7 development blocks together) of the Bundelkhand region.

predictions arising from actual temporal changes in soil properties versus model uncertainties poses a significant challenge. While evaluating the temporal applicability of trained DRS model studies are limited, a quantitative assessment of the degree to which a calibrated (or cross-validated) DRS model can effectively be applicable to test soil properties in new samples is rarely addressed in the DRS literature. Specifically, how many new samples can be tested with what error threshold is not addressed in the DRS literature although *PRED*(*T*) is readily used for assessing models in software engineering (Shepperd and MacDonell, 2012).

Our study addressed some of the above research gaps by exploring the applicability of calibrated DRS models for the estimation of 17 soil properties measured at two different time periods. Our study site covered 8 development blocks spreading across 7 districts of the Bundelkhand region in Uttar Pradesh, India. Representative samples were collected from this region with varying sampling densities through stratified sampling. Sampling locations in Banda district were evenly distributed between two sampling campaigns of 2018 and 2021; sampling densities varied significantly from 2018 to 2021 at Jalaun and Hamirpur. Through preliminary modelling studies, we observed the Cubist model to be effective in estimating several soil parameters and their ratings in the DRS approach. In addition to classical evaluation metrices such as R^2 and RMSEs, we also used *PRED*(30) values to assess the effectiveness of the DRS approach when a set of new samples are to be analysed.

With the diverse set of soil samples from multiple sites, we considered four modelling scenarios to evaluate the efficacy of DRS approach: site-specific testing, spiking of calibration datasets, localizing to finer spatial scales, and model applicability to spatially- and temporally-independent test dataset. Results indicated mixed success for the calibrated DRS models in estimating soil parameters in test datasets developed from our sampled regions. Our results showed that exchangeable Ca and Mg, clay and fine sand contents were well estimated across most scenarios with *PRED*(30) values exceeding 75 % (Table 6), particularly, in regions with finer-textured soils and also in regional-scale dataset. There is a consistent performance in the estimation of SOC contents with R^2 and *PRED*(30) values ranging from 0.54 to 0.79 and from 52 % to 86 % (Table 6), respectively. Zayani et al. (2023) also obtained R^2 value ranging from 0.65 to 0.85 using the 10 % of the samples spiked and recalibrated model (Table 1). For the clay content, our models showed better modelling performance (R^2: 0.54 to 0.85) than those of Tsatsoulis et al. (2023), who reported R^2 value ranging from 0.50 to 0.59 (Table 1). However, some micronutrients and coarse sand contents showed poor estimation accuracy, especially, in coarse-textured soils such as those of

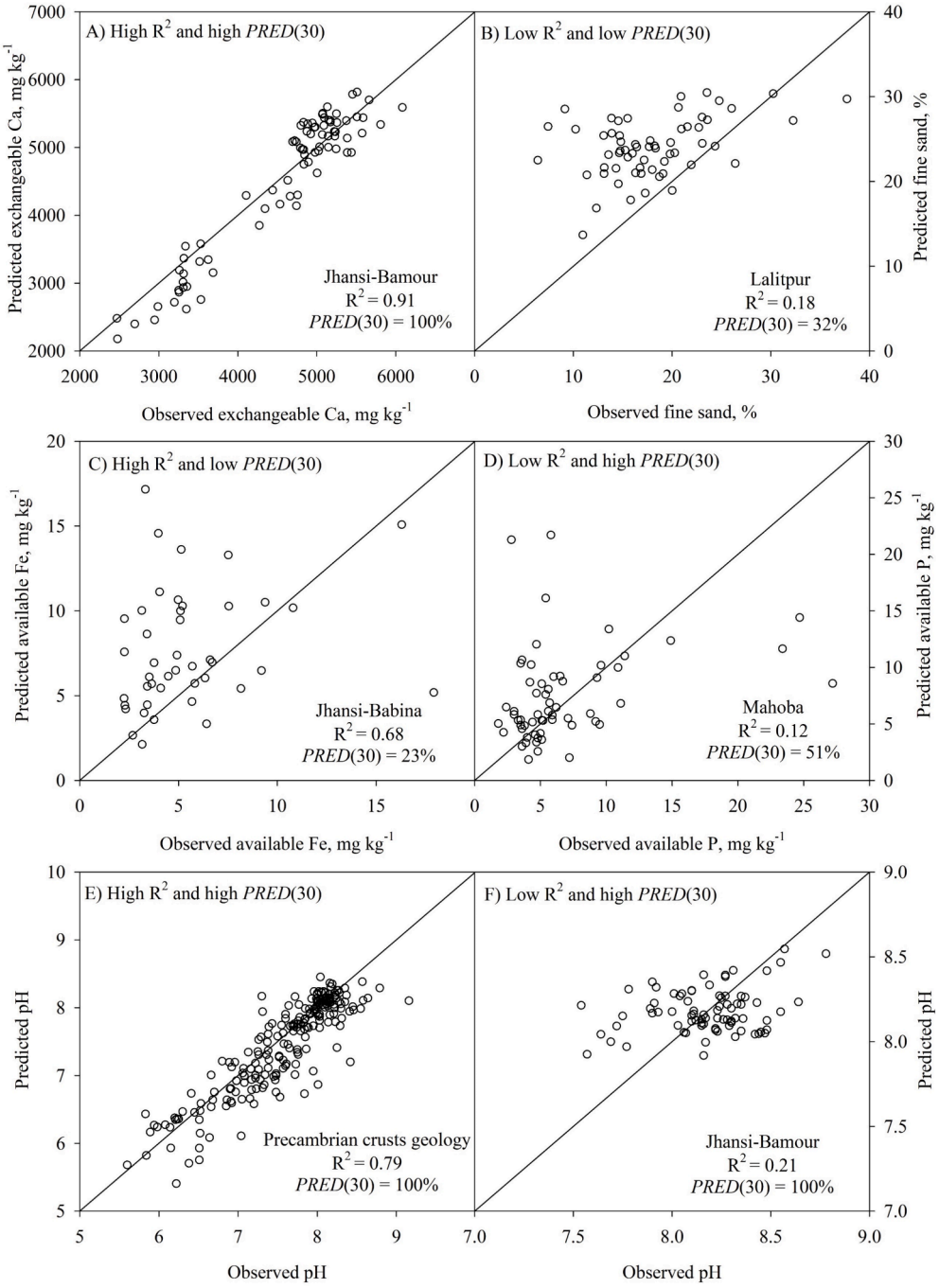

Fig. 11. Scatter plots showing observed vs. predicted values of selected soil properties from selected modelling scenarios to compare the coefficient of determination (R^2) and percentage relative error deviation (*PRED*) at 30% threshold.

Lalitpur and Jhansi-Babina. Nevertheless, the STCR rating accuracy showed a close match with those of conventional soil testing. Results shown in Table S10 clearly suggested that with additional investment through spiking an existing calibration dataset can lead to improvement in the accuracy of the DRS approach for estimating 7–10 out of 17 soil parameters with > 80 % SRA values. Specifically, the improvements are seen in critical soil parameters such as SOC contents and some of the macro- and micro-nutrients. Although our results are similar to some of the previous studies (Brown, 2007; Guerrero et al., 2010; Guerrero et al., 2014; Sankey et al., 2008; Hong et al., 2018), spiking is often shown to produce no significant improvement in predicting soil properties compared to no-spiking scenarios (Wetterlind and Stenberg, 2010; Goǵe et al., 2014). More recently, Ng et al. (2022) showed that local models built with a small fraction of the test data may also be useful to estimate soil properties in a specific dataset. Therefore, we examined the local model of Ng et al. (2022) for our test data set of 2021 (T_{2021}) using 20 % of the cLHS-selected data. For all our datasets, this amounted to have 20 to 30 calibration samples as suggested in Ng et al. (2022). Fig. 12 shows the resulting R^2 and RMSE ratios for both spiked and local model scenarios in our datasets. Large improvement in R^2 values for the spiked data set compared to the local model may be seen for soil properties such as coarse sand, fine sand, pH, SOC contents, exchangeable K, Mg, available B, Fe, and Cu (Fig. 12A) while the spiking approach always outperformed the local model which may be seen from reduced RMSE ratio (Fig. 12B). Specifically, the boxplot for the RMSE ratio was below 1.0 for both the geology-specific and regional-scale datasets suggesting

Table 6
The percentage relative error deviation at 30% error threshold values were obtained using best performing modelling approach for each development block, geology-specific, and regional-scale datasets.

Soil properties	Lalitpur	Jhansi-Bhabina	Mahoba	Jalaun	Hamirpur	Banda	Chitrakoot	Jhansi-Bamour	PCG	QSG	RS
Coarse sand, %	86	75	45	33	26	20	50	42	65	44	51
Fine sand, %	32	75	90	89	98	90	88	90	76	90	84
Clay, %	66	47	88	95	93	88	86	94	75	91	84
pH	100	100	100	100	100	100	100	100	100	100	100
EC, dS m^{-1}	26	40	67	37	71	58	55	35	40	56	49
SOC, %	52	53	75	61	86	83	75	81	66	80	70
Av. P	32	32	51	53	50	33	27	42	34	43	43
Ex. K	19	35	69	49	71	75	62	59	48	66	53
Ex. Ca	60	77	100	99	100	93	99	100	81	97	93
Ex. Mg	40	75	85	93	93	100	90	89	85	91	86
Av. S	16	40	48	29	55	53	53	33	40	36	32
Av. Zn	23	33	34	24	31	48	64	46	36	46	42
Av. B	35	53	61	88	88	55	40	77	53	66	62
Av. Fe	31	23	52	67	45	70	78	46	32	62	52
Av. Cu	40	53	82	92	71	90	84	76	62	83	73
Av. Mn	43	58	67	25	36	43	56	41	48	46	47
Ex. Na	36	38	25	75	57	23	37	22	44	49	47

PCG: Precambrian crusts geology; QSG: Quaternary sediments geology; RS: regional-scale; EC: electrical conductivity; SOC: soil organic carbon; Av.: available, Ex.: exchangeable. All nutrient contents are in mg kg^{-1}.

that the spiked models show better performance than the local models. We recognise that these results are data-driven and there may be scenarios where local model is adequate. In our case, Fig. 12 shows a clear advantage of spiking approach over the local models. Thus, our results suggest that local-scale datasets (e.g., development block) should carefully be combined to form large-scale datasets (e.g., geology-specific and regional-scale), which should then be spiked to train a robust DRS model. Such a model should, in turn, be applied to estimate soil properties in local datasets (Table S10).

Our analysis showed that the spectral domains of the calibration datasets and the ranges of soil attributes significantly influence the applicability of the trained DRS models in addition to environmental factors (Minasny et al., 2009; Grunwald et al., 2018; Hong et al., 2018), the relationship between soil chromophores and non-chromophores (Sarathjith et al., 2016), and the choice of chemometric modelling approaches. For instance, regions with predominantly coarse-textured soils, such as Lalitpur, often exhibited poor estimation accuracy for various soil properties compared to regions with clay or clay loam textures (Table S10). This discrepancy arises because features associated with specific soil properties, such as SOC contents, can be masked or distorted by other soil components such as iron oxides and secondary clays, which are common in soils (Hunt, 1989; Clark, 1999). This issue poses a critical challenge in VNIR modelling, where soil properties such as texture, nutrient content, and specific mineral fractions may interfere with the accurate prediction of targeted properties (Grunwald et al., 2018). Moreover, variations in soil management practices followed by individual farmers and discrepancies in sampling locations relative to calibration sites may contribute to the variability in soil properties captured by soil spectra. This can lead to some soil samples lying outside the spectral calibration domain (Fig. 3). Furthermore, the diversity in soil formation environments, influenced by geographical origins and parent materials, results in area-specific spectral responses of soil VNIR spectra (Ramirez-Lopez et al., 2013; Shi et al., 2015; Viscarra Rossel et al., 2016; Hong et al., 2018). Minasny et al. (2009) have observed that limited portability of MIR spectra-based SOC prediction models among different regions in Australia—Queensland, New South Wales, and Victoria because of the differences in parent material and climatic conditions under which soils formed. We also observed parent material significantly influencing the applicability of the trained DRS models. For example, localizing geology-specific models (scenario 3) performed better than the regional-scale models in estimating soil properties in Lalitpur, Jhansi-Babina, and Hamirpur. The Precambrian crust rock system in these three sites are dominantly granitic in nature while the regional dataset would have a mixed mineralogy because of the diverse mineral phases expected in sedimentary alluvium in the northern part of the Bundelkhand region. With dominant mineral phases, soil samples from the Precambrian rock system may be having strong spectral signatures leading to better estimation accuracies for the calibrated models; Fig. 3A and 3B show that the PCG samples were generally more reflective than those of the QSG samples. Our results also suggested that the applicability of calibrated DRS models on temporal dataset is relatively more reliable for soil chromophores especially when the spectral domains of the test datasets are similar to those of the calibration data. Moreover, our results also showed that temporal applicability is more reliable for evaluating DRS-based STCR ratings for almost all the soil parameters tested in typical agricultural soil testing applications. Results of the applicability of trained models for SOC contents suggest that SOC can be reliably estimated in new samples using the DRS approach. While large-scale and frequent monitoring of SOC contents is critical to meeting several SDGs and emerging carbon markets the ability to frequently monitor micronutrient concentrations through the DRS approaches has the potential to make micronutrient application as a routine practice in farming. The later has the potential to alleviate multiple burdens of malnutrition by carefully tailoring micronutrient management in agriculture. Ability to accurately assess soil texture through the DRS approach can also enhance our capability in geo-hydrological modeling because soil texture is an essential component of earth systems models and many of our national soil health efforts often lack this important dataset. In our study, we did not have any soil hydraulic property data although the DRS approach is also known to be useful for estimating this important soil parameter (Santra et al., 2009). The success of the DRS approach in independent test dataset in such proximal mode of operation in our study should also be replicated for the hyperspectral remote sensing (HRS) applications given that recent studies have shown HRS data may be used for estimating multiple soil parameters (Majeed et al., 2023b) and composite soil parameters such as soil quality index (Majeed and Das, 2024).

5. Conclusion

Evaluating the applicability of calibrated models across spatial and temporal boundaries is an essential step to promote the DRS approach as a compliment to wet-chemistry based soil testing from a commercial standpoint. With this overall objective, a total of 1,112 and 607 soil samples were collected from eight development blocks belonging to seven districts of Bundelkhand region in 2018 and 2021, respectively. Collected soil samples did not share the same coordinates providing spatial discreteness in samples. A series of modelling studies involving

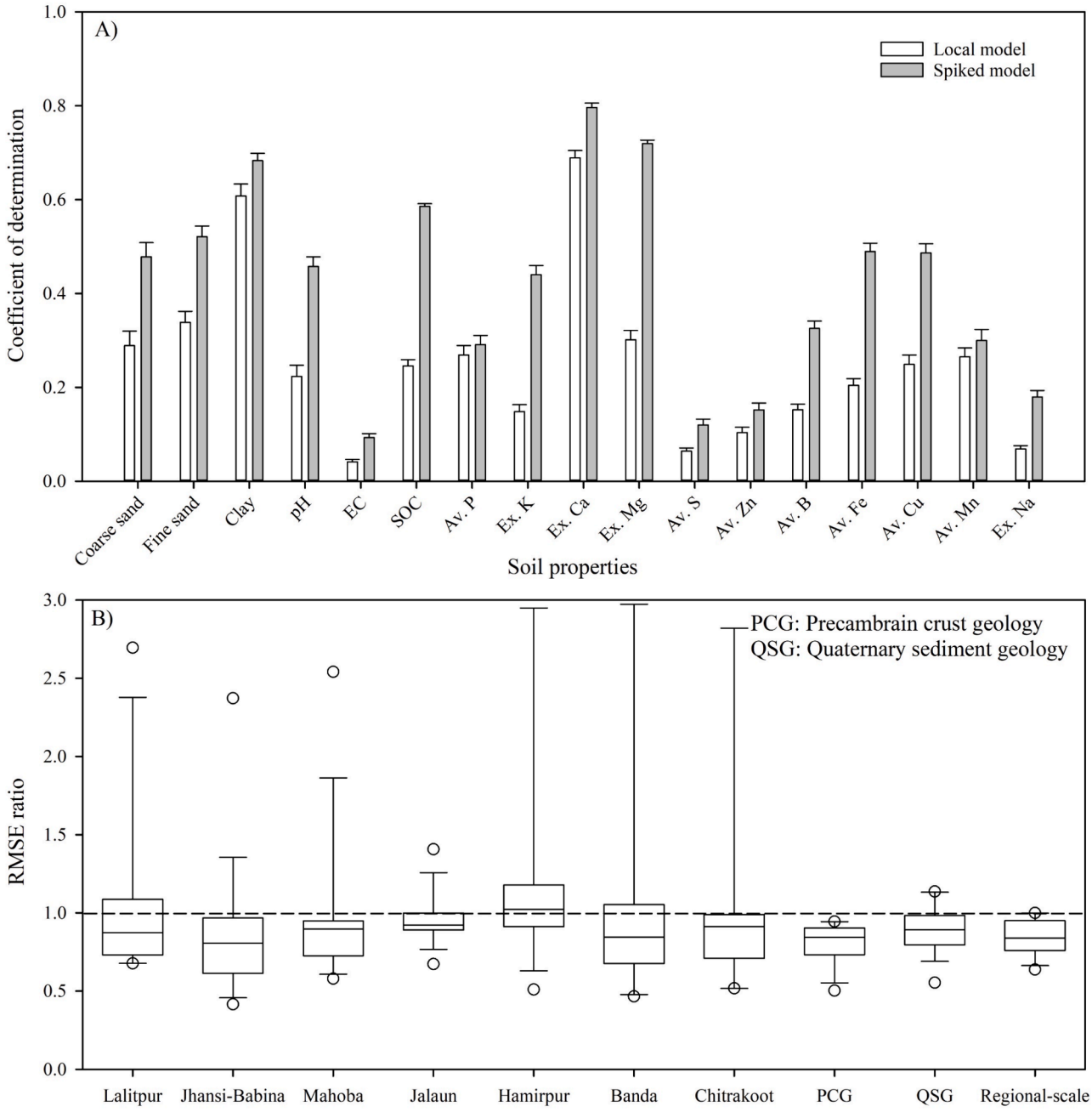

Fig. 12. Bar plots showing the coefficient of determination and their standard error of mean values (A) and box plots showing the root-mean-square error (RMSE) ratio (B) for the spiking approach and local modelling approach (Ng et al., 2022) using the site-specific, geology-specific and regional-scale datasets. The RMSE ratios were obtained by dividing the RMSE values of spiked models by the RMSE values of local models.

applicability of calibrated Cubist models in both spatially- and temporally-independent test datasets showed that most of the soil chromophores could be estimated in test samples with moderate to good estimation accuracy supporting their temporal applicability. Specifically, our results showed that oil properties such as exchangeable Ca, Mg, clay and fine sand contents may be well estimated in independent test samples with R^2 values exceeding 0.6. Moreover, SOC contents showed moderate to excellent estimation accuracy in all our datasets with $R^2 > 0.5$. However, most of the soil non-chromophores were poorly estimated in the test samples using the DRS approach. A significant result of our study is that the STCR ratings for several soil parameters showed excellent estimation accuracy in almost all our test datasets.

Estimation errors also substantially decreased (to the tune of 88 %) when 20 % of the test samples were selected through the cLHS algorithm for spiking the training data. Spiking also improved the STCR rating accuracies to the tune of 48 % of the cases. When tested against a spatially- and temporally-independent dataset, the calibrated models using geology-specific and regional-scale training datasets resulted in excellent STCR rating accuracies; 8 out 13 soil parameters showed similar STCR ratings in > 85 % of samples both in the DRS-based and wet chemistry-based soil testing approaches. Overall, the spectral domain, soil texture, parent materials, and the relationship between the soil chromophores and non-chromophores had a significant impact on the applicability of trained DRS models for estimating the soil properties. These results suggest that the DRS approach may be used to predict the soil parameters for samples collected at different locations and in different time periods using existing validated models. Specifically, similar STCR ratings for DRS-estimated soil parameters to those with

conventional soil testing suggest that nutrient recommendations may safely be made using DRS approach. This offers cost savings for farmers and has the potential to improve current trends in nutrient recommendations and usage. Deep learning, deep transfer learning, and instant transfer learning are not yet explored in this study because a small number of calibration data did not permit us to build such models, which may be explored in future studies. Extending this research to the DRS applications from hyperspectral remote sensing data may also provide opportunities to implement the precision farming approach at various spatial scales practically.

CRediT authorship contribution statement

Naveen K. Purushothaman: Writing – original draft, Software, Methodology, Data curation, Conceptualization. **Kaushal K. Garg:** . **A. Venkataradha:** Writing – review & editing, Resources. **K.H. Anantha:** Writing – review & editing, Resources, Investigation. **Ramesh Singh:** . **M.L. Jat:** Writing – review & editing, Project administration. **Bhabani S. Das:** Writing – review & editing, Supervision, Conceptualization.

Declaration of competing interest

The authors declare that they have no known competing financial interests or personal relationships that could have appeared to influence the work reported in this paper.

Data availability

The authors do not have permission to share data.

Acknowledgements

We thankfully acknowledge the funding support received from Rastriya Krishi Vikas Yojana (RKVY) through Department of Agriculture, Government of Uttar Pradesh for undertaking Doubling Farmers' Income (DFI) initiative in Uttar Pradesh Bundelkhand region, Central India. Support in spectral data collection by Dr. Israr Majeed is thankfully acknowledged. The first author acknowledges the Prime Minister's Research Fellowship (PMRF), Round 10 (lateral entry) for his PhD research.

Appendix A. Supplementary data

Supplementary data to this article can be found online at https://doi.org/10.1016/j.geoderma.2024.117012.

References

Ahmadi, A., Emami, M., Daccache, A., He, L., 2021. Soil properties prediction for precision agriculture using visible and near-infrared spectroscopy: a systematic review and meta-analysis. Agronomy 11 (3), 433. https://doi.org/10.3390/agronomy11030433.

Allen, D.E., Singh, B.P., Dalal, R.C., 2011. Soil Health Indicators Under Climate Change: A Review of Current Knowledge. In: Singh, B., Cowie, A., Chan, K. (Eds.), Soil Health and Climate Change. Soil Biol., vol 29, Springer, Berlin, Heidelberg. Doi: 10.1007/978-3-642-20256-8_2.

Bagnall, D.K., Shanahan, J.F., Flanders, A., Morgan, C.L., Honeycutt, C.W., 2021. Soil health considerations for global food security. Agronomy J. 113 (6), 4581–4589. https://doi.org/10.1002/agj2.20783.

Barbetti, R., Palazzi, F., Chiarabaglio, P.M., Fondon, C.L., Rizza, D., Rocci, A., Grignani, C., Zavattaro, L., Moretti, B., Fantappié, M. and Monaco, S., 2023, November. Can soil organic carbon in long–term experiments be detected using Vis-NIR spectroscopy?. In 2023 IEEE International Workshop on Metrology for Agriculture and Forestry (MetroAgriFor) (pp. 154-159). IEEE. Doi: 10.1109/MetroAgriFor58484.2023.10424077.

Barnes, R.J., Dhanoa, M.S., Lister, S.J., 1989. Standard normal variate transformation and de-trending of near-infrared diffuse reflectance spectra. Appl. Spectrosc. 43 (5), 772–777. https://doi.org/10.1366/0003702894202201.

Bellinaso, H., Demattê, J.A.M., Romeiro, S.A., 2010. Soil spectral library and its use in soil classification. Revista Brasileira De Ciência Do Solo 34, 861–870. https://doi.org/10.1590/S0100-06832010000300027.

Bellon-Maurel, V., Fernandez-Ahumada, E., Palagos, B., Roger, J.M., McBratney, A., 2010. Critical review of chemometric indicators commonly used for assessing the quality of the prediction of soil attributes by NIR spectroscopy. TrAC – Trends Anal. Chem. 29 (9), 1073–1081. https://doi.org/10.1016/j.trac.2010.05.006.

Ben-Dor, E., Banin, A., 1995. Near-infrared analysis as a rapid method to simultaneously evaluate several soil properties. Soil Sci. Soc. Am. J. 59 (2), 364–372. https://doi.org/10.2136/sssaj1995.03615995005900020014x.

Blöschl, G., Sivapalan, M., 1995. Scale issues in hydrological modelling: a review. Hydrol. Process. 9 (3–4), 251–290. https://doi.org/10.1002/hyp.3360090305.

Brown, D.J., 2007. Using a global VNIR soil-spectral library for local soil characterization and landscape modeling in a 2nd-order Uganda watershed. Geoderma 140 (4), 444–453. https://doi.org/10.1016/j.geoderma.2007.04.021.

Brunet, D., Barthès, B.G., Chotte, J.L., Feller, C., 2007. Determination of carbon and nitrogen contents in Alfisols, Oxisols and Ultisols from Africa and Brazil using NIRS analysis: effects of sample grinding and set heterogeneity. Geoderma 139 (1–2), 106–117. https://doi.org/10.1016/j.geoderma.2007.01.007.

Clark, R.N., 1999. Spectroscopy of rocks and minerals, and principles of spectroscopy. In: Rencz, A.N. (Ed.), Manual of Remote Sensing, Volume 3. Remote Sensing for the Earth Sciences, John Wiley and Sons, New York, pp. 3–58.

Coblinski, J.A., Giasson, É., Demattê, J.A., Dotto, A.C., Costa, J.J.F., Vašát, R., 2020. Prediction of soil texture classes through different wavelength regions of reflectance spectroscopy at various soil depths. Catena 189, 104485.

Conte, S.D., Dunsmore, H.E., Shen, Y.E., 1986. Software engineering metrics and models. Benjamin-Cummings Publishing Co., Inc.

Dangal, S., Sanderman, J., Wills, S., Ramirez-Lopez, L., 2019. Accurate and precise prediction of soil properties from a large mid-infrared spectral library. Soil Systems 3, 11. https://doi.org/10.3390/soilsystems3010011.

de Souza Bahia, A.S.R., Marques, J., La Scala, N., Pellegrino Cerri, C.E., Camargo, L.A., 2017. Prediction and mapping of soil attributes using diffuse reflectance spectroscopy and magnetic susceptibility. Soil Sci. Soc. Am. J. 81 (6), 1450–1462. https://doi.org/10.2136/sssaj2017.06.0206.

Dorantes, M.J., Fuentes, B.A., Miller, D.M., 2022. Calibration set optimization and library transfer for soil carbon estimation using soil spectroscopy-A review. Soil Sci. Soc. Am. J. 86 (4), 879–903. https://doi.org/10.1002/saj2.20435.

Editorial, N., 2020. Ending hunger: Science must stop neglecting smallholder farmers. Nature 586, 336.

Ekka, P., Patra, S., Upreti, M., Kumar, G., Kumar, A., Saikia, P., 2023. Land Degradation and Its Impacts on Biodiversity and Ecosystem Services. In: Raj, A., Jhariya, M.K., Banerjee, A., Nema, S., K. Bargali (Eds.), In Land and Environmental Management through Forestry. Doi: 10.1002/9781119910527.ch4.

Franceschini, M.H.D., Demattê, J.A.M., Kooistra, L., Bartholomeus, H., Rizzo, R., Fongaro, C.T., Molin, J.P., 2018. Effects of external factors on soil reflectance measured on-the-go and assessment of potential spectral correction through orthogonalisation and standardisation procedures. Soil Tillage Res. 177, 19–36. https://doi.org/10.1016/j.still.2017.10.004.

Garg, K.K., Singh, R., Anantha, K.H., Singh, A.K., Akuraju, V.R., Barron, J., Dev, I., Tewari, R.K., Wani, S.P., Dhyani, S.K., Dixit, S., 2020. Building climate resilience in degraded agricultural landscapes through water management: a case study of Bundelkhand region, Central India. J. Hydrol. 591, 125592 https://doi.org/10.1016/j.jhydrol.2020.125592.

Gholizadeh, A., Saberioon, M., Carmon, N., Boruvka, L., Ben-Dor, E., 2018. Examining the performance of PARACUDA-II data-mining engine versus selected techniques to model soil carbon from reflectance spectra. Remote Sensing 10 (8), 1172. https://doi.org/10.3390/rs10081172.

Goǵe, F., Gomez, C., Jolivet, C., Joffre, R., 2014. Which strategy is best to predict soil properties of a local site from a national Vis–NIR database? Geoderma 213, 1–9. https://doi.org/10.1016/j.geoderma.2013.07.016.

Gomez, C., Coulouma, G., 2018. Importance of the spatial extent for using soil properties estimated by laboratory VNIR/SWIR spectroscopy: examples of the clay and calcium carbonate content. Geoderma 330, 244–253. https://doi.org/10.1016/j.geoderma.2018.06.006.

Grunwald, S., Congrong, Y.U., Xiong, X., 2018. Transferability and scalability of soil total carbon prediction models in Florida, USA. Pedosphere 28 (6), 856–872. https://doi.org/10.1016/S1002-0160(18)60048-7.

Guerrero, C., Zornoza, R., Gómez, I., Mataix-Beneyto, J., 2010. Spiking of NIR regional models using samples from target sites: Effect of model size on prediction accuracy. Geoderma 158 (1–2), 66–77. https://doi.org/10.1016/j.geoderma.2009.12.021.

Guerrero, C., Stenberg, B., Wetterlind, J., Viscarra Rossel, R.A., Maestre, F.T., Mouazen, A.M., Zornoza, R., Ruiz-Sinoga, J.D., Kuang, B., 2014. Assessment of soil organic carbon at local scale with spiked NIR calibrations: effects of selection and extra-weighting on the spiking subset. Europ. J. Soil Sci. 65 (2), 248–263. https://doi.org/10.1111/ejss.12129.

Hanway, J.J., Heidel, H., 1952. Soil analysis methods as used in Iowa state college soil testing laboratory. Iowa Agric. 57, 1–31.

Havlin, J.L., Tisdale, S.L., Nelson, W.L., Beaton, J.D., 2014. Soil Fertility and Nutrient Management: An Introduction to Nutrient Management, 8th edition. Pearson, Upper Saddle River, NJ, p. 505.

Hong, Y., Chen, Y., Zhang, Y., Liu, Y., Liu, Y., Yu, L., Liu, Y., Cheng, H., 2018. Transferability of Vis-NIR models for soil organic carbon estimation between two study areas by using spiking. Soil Sci. Soc. Am. J. 82 (5), 1231–1242. https://doi.org/10.2136/sssaj2018.03.0099.

Huang, S., Zhang, X., Chen, N., Ma, H., Fu, P., Dong, J., Gu, X., Nam, W.H., Xu, L., Rab, G., Niyogi, D., 2022. A novel fusion method for generating surface soil moisture data with high accuracy, high spatial resolution, and high spatio-temporal continuity. Water Resour. Res. 58 (5) https://doi.org/10.1029/2021WR030827 pp. e2021WR030827.

Hunt, G.R., 1989. Spectroscopic properties of rocks and minerals.In Carmichael R S (ed.) Practical Handbook of Physical Properties of Rocks and Minerals. CRC Press, Taylor & Francis, Boca Raton. pp. 295–385.
Idri, A., Azzahra, A.F., Abran, A., 2015. Analogy-based software development effort estimation: a systematic mapping and review. Informat. Softw. Technol. 58, 206–230. https://doi.org/10.1016/j.infsof.2014.07.013.
Idri, A., Abnane, I., Abran, A., 2018. Evaluating Pred (p) and standardized accuracy criteria in software development effort estimation. J. Softw.: Evolut. Process 30 (4), e1925.
Islam, K., McBratney, A., Singh, B., 2005. Rapid estimation of soil variability from the convex hull biplot area of topsoil ultra-violet, visible and near-infrared diffuse reflectance spectra. Geoderma 128 (3–4), 249–257. https://doi.org/10.1016/j.geoderma.2005.04.007.
Jatav, S.S., 2022. Rainfall and temperature perception among farmers in india: a study of bundelkhand region. J. Sustain. Environ. Manag. 1 (3), 321–331.
Jiang, C., Zhang, H., Zhao, L., Yang, Z., Wang, X., Yang, L., Wen, M., Geng, S., Zeng, Q., Wang, J., 2020. Unfolding the effectiveness of ecological restoration programs in combating land degradation: achievements, causes, and implications. Sci. Total Environ. 748, 141552 https://doi.org/10.1016/j.scitotenv.2020.141552.
Keren, R., 1996. Boron. In: Sparks, D. L., Page, A. L. (Eds.), Methods of soil analysis, part 3 chemical methods. Soil Sci. Soc. Am. and Am. Soc. Agron. (pp. 603–626).
Kuhn, M., 2008. Building Predictive Models in R Using the caret Package. J. Statist. Softw. 28 (5), 1–26. https://doi.org/10.18637/jss.v028.i05.
Kuhn, M., Quinlan, R., 2023. Cubist: rule- and instance-based regression modeling. R package version 0.4.2.1. https://CRAN.R-project.org/package=Cubist.
Kumar, D., Ranjan, R., Meena, M.K., Yadav, R.S., Gupta, G., Jinger, D., Yadav, D., Pramanik, M., 2021. Exploring Conservation Agricultural Practices in Bundelkhand Region, Central India. In: Jayaraman, S., Dalal, R.C., Patra, A.K., Chaudhari, S.K. (Eds.), Conservation Agriculture: A Sustainable Approach for Soil Health and Food Security. Springer, Singapore. https://doi.org/10.1007/978-981-16-0827-8_9.
Laborde, D., Murphy, S., Parent, M., Porciello, J., Smaller, C., 2020. Ceres2030: Sustainable Solutions to End Hunger-Summary Report. Cornell University, IFPRI and IISD.
Lal, R., Bouma, J., Brevik, E., Dawson, L., Field, D.J., Glaser, B., Hatano, R., Hartemink, A.E., Kosaki, T., Lascelles, B., Monger, C., 2021. Soils and sustainable development goals of the United Nations: An International Union of Soil Sciences perspective. Geoderma Regional 25, e00398.
Lal, R., 2011. Soil Health and Climate Change: An Overview. In: Singh, B., Cowie, A., Chan, K. (Eds.), Soil Health and Climate Change. Soil Biol., vol. 29, Springer, Berlin, Heidelberg. Doi: 10.1007/978-3-642-20256-8_1.
Lal, R., 2017. Improving soil health and human protein nutrition by pulses-based cropping systems. In: Sparks, D. L. (Eds.). Adv. Agron. 145, pp.167-204. Doi: 10.1016/bs.agron.2017.05.003.
Leal Filho, W., Nagy, G.J., Setti, A.F.F., Sharifi, A., Donkor, F.K., Batista, K., Djekic, I., 2023. Handling the impacts of climate change on soil biodiversity. Sci. Total Environ. 869, 161671 https://doi.org/10.1016/j.scitotenv.2023.161671.
Li, H., Li, Y., Yang, M., Chen, S., Shi, Z., 2022a. Strategies for efficient estimation of soil organic content at the local scale based on a national spectral database. Land Degrad. Dev. 33 (10), 1649–1661. https://doi.org/10.1002/ldr.4223.
Li, S., Viscarra Rossel, R.A., Webster, R., 2022b. The cost-effectiveness of reflectance spectroscopy for estimating soil organic carbon. Eur. J. Soil Sci. 73 (1), e13202.
Liu, Y., Jiang, Q., Fei, T., Wang, J., Shi, T., Guo, K., Li, X., Chen, Y., 2014. Transferability of a visible and near-infrared model for soil organic matter estimation in riparian landscapes. Remote Sensing 6 (5), 4305–4322. https://doi.org/10.3390/rs6054305.
Liu, Y., Shi, Z., Zhang, G., Chen, Y., Li, S., Hong, Y., Shi, T., Wang, J., Liu, Y., 2018. Application of spectrally derived soil type as ancillary data to improve the estimation of soil organic carbon by using the Chinese soil vis-NIR spectral library. Remote Sens. 10 (11), 1747. https://doi.org/10.3390/rs10111747.
Lobsey, C.R., Viscarra Rossel, R.A., Roudier, P., Hedley, C.B., 2017. RS-local data-mines information from spectral libraries to improve local calibrations. Eur. J. Soil Sci. 68 (6), 840–852. https://doi.org/10.1111/ejss.12490.
Lucà, F., Conforti, M., Castrignanò, A., Matteucci, G., Buttafuoco, G., 2017. Effect of calibration set size on prediction at local scale of soil carbon by Vis-NIR spectroscopy. Geoderma 288, 175–183. https://doi.org/10.1016/j.geoderma.2016.11.015.
Luce, M.S., Ziadi, N., Viscarra Rossel, R.A., 2022. GLOBAL-LOCAL: a new approach for local predictions of soil organic carbon content using large soil spectral libraries. Geoderma 425, 116048. https://doi.org/10.1016/j.geoderma.2022.116048.
Ludwig, B., Murugan, R., Parama, V.R., Vohland, M., 2019. Accuracy of estimating soil properties with mid-infrared spectroscopy: Implications of different chemometric approaches and software packages related to calibration sample size. Soil Sci. Soc. Am. J. 83 (5), 1542–1552. https://doi.org/10.2136/sssaj2018.11.0413.
Majeed, I., Das, B.S., 2024. Large-scale mapping of soil quality index in different land uses using airborne hyperspectral data. IEEE Trans. Geosci. Remote Sens. 62, 1–12. https://doi.org/10.1109/TGRS.2024.3360334.
Majeed, I., Garg, K.K., Venkataradha, A., Purushothaman, N.K., Roy, S., Reddy, N.N., Singh, R., Anantha, K.H., Dixit, S., Das, B.S., 2023a. Diffuse reflectance spectroscopy (DRS) for rapid soil testing and soil quality assessment in smallholder farms. Eur. J. Soil Sci. 74 (2), e13358.
Majeed, I., Purushothaman, N.K., Chakraborty, P., Panigrahi, N., Vasava, H.B., Das, B.S., 2023b. Estimation of soil and crop residue parameters using AVIRIS-NG hyperspectral data. Int. J. Remote Sens. 44 (6), 2005–2038. https://doi.org/10.1080/01431161.2023.2195570.
McBride, M.B., 2022. Estimating soil chemical properties by diffuse reflectance spectroscopy: Promise versus reality. Eur. J. Soil Sci. 73 (1), e13192.
Minasny, B., McBratney, A.B., 2006. A conditioned Latin hypercube method for sampling in the presence of ancillary information. Comput. Geosci. 32 (9), 1378–1388. https://doi.org/10.1016/j.cageo.2005.12.009.
Minasny, B., McBratney, A.B., 2008. Regression rules as a tool for predicting soil properties from infrared reflectance spectroscopy. Chemom. Intell. Lab. Syst. 94 (1), 72–79. https://doi.org/10.1016/j.chemolab.2008.06.003.
Minasny, B., Tranter, G., McBratney, A.B., Brough, D.M., Murphy, B.W., 2009. Regional transferability of mid-infrared diffuse reflectance spectroscopic prediction for soil chemical properties. Geoderma 153 (1–2), 155–162. https://doi.org/10.1016/j.geoderma.2009.07.021.
Minasny, B., McBratney, A.B., Bellon-Maurel, V., Roger, J.M., Gobrecht, A., Ferrand, L., Joalland, S., 2011. Removing the effect of soil moisture from NIR diffuse reflectance spectra for the prediction of soil organic carbon. Geoderma 167, 118–124. https://doi.org/10.1016/j.geoderma.2011.09.008.
Moloney, J.P., Malone, B.P., Karunaratne, S., Stockmann, U., 2023. Leveraging large soil spectral libraries for sensor-agnostic field condition predictions of several agronomically important soil properties. Geoderma 439, 116651. https://doi.org/10.1016/j.geoderma.2023.116651.
Morais, T.G., Tufik, C., Rato, A.E., Rodrigues, N.R., Gama, I., Jongen, M., Serrano, J., Fangueiro, D., Domingos, T., Teixeira, R.F., 2021. Estimating soil organic carbon of sown biodiverse permanent pastures in Portugal using near infrared spectral data and artificial neural networks. Geoderma 404, 115387. https://doi.org/10.1016/j.geoderma.2021.115387.
Ng, W., Minasny, B., Malone, B., Filippi, P., 2018. In search of an optimum sampling algorithm for prediction of soil properties from infrared spectra. PeerJ 6, e5722.
Ng, W., Minasny, B., Malone, B.P., Sarathjith, M.C., Das, B.S., 2019a. Optimizing wavelength selection by using informative vectors for parsimonious infrared spectra modelling. Comput. Electron. Agric. 158, 201–210. https://doi.org/10.1016/j.compag.2019.02.003.
Ng, W., Minasny, B., Montazerolghaem, M., Padarian, J., Ferguson, R., Bailey, S., McBratney, A.B., 2019b. Convolutional neural network for simultaneous prediction of several soil properties using visible/near-infrared, mid-infrared, and their combined spectra. Geoderma 352, 251–267. https://doi.org/10.1016/j.geoderma.2019.06.016.
Ng, W., Minasny, B., Jones, E., McBratney, A., 2022. To spike or to localize? Strategies to improve the prediction of local soil properties using regional spectral library. Geoderma 406, 115501. https://doi.org/10.1016/j.geoderma.2021.115501.
Oliver, M.A., Gregory, P.J., 2015. Soil, food security and human health: a review. Eur. J. Soil Sci. 66 (2), 257–276. https://doi.org/10.1111/ejss.12216.
Olsen, S. R., Sommers, L. E., 1982. Phosphorus. In: Page, A. L., Miller, R. H., Keeney D. R. (Eds.), in methods of soil analysis. Part II (2nd ed., pp. 403–430). Am. Soc. Agron. and Soil Sci. Soc. Am.
O'rourke, S.M., Stockmann, U., Holden, N.M., McBratney, A.B., Minasny, B., 2016. An assessment of model averaging to improve predictive power of portable vis-NIR and XRF for the determination of agronomic soil properties. Geoderma 279, 31–44. https://doi.org/10.1016/j.geoderma.2016.05.005.
Quinlan, J.R., 1993. C4.5: Programs for Machine Learning. Morgan Kaufmann Publishers Inc., San Mateo, California.
R Core Team., 2023. R: A language and environment for statistical computing. R Foundation for Statistical Computing, Vienna, Austria https://www.R-project.org/.
Ramirez-Lopez, L., Behrens, T., Schmidt, K., Stevens, A., Demattê, J.A.M., Scholten, T., 2013. The spectrum-based learner: A new local approach for modeling soil vis–NIR spectra of complex datasets. Geoderma 195, 268–279. https://doi.org/10.1016/j.geoderma.2012.12.014.
Ramirez-Lopez, L., Schmidt, K., Behrens, T., Van Wesemael, B., Demattê, J.A., Scholten, T., 2014. Sampling optimal calibration sets in soil infrared spectroscopy. Geoderma 226, 140–150. https://doi.org/10.1016/j.geoderma.2014.02.002.
Reeves, J.B., McCarty, G.W., Meisinger, J.J., 1999. Near infrared reflectance spectroscopy for the analysis of agricultural soils. J. near Infrared Spectrosc. 7 (3), 179–193.
Ricciardi, V., Mehrabi, Z., Wittman, H., James, D., Ramankutty, N., 2021. Higher yields and more biodiversity on smaller farms. Nat. Sustain. 4 (7), 651–657. https://doi.org/10.1038/s41893-021-00699-2.
Rickson, R., Deeks, L., Corstanje, R., Newell-Price, P., Kibblewhite, M., Chambers, B., Bellamy, P., Holman, I., James, I., Jones, R., Kechavarsi, C., Mouazen, A., Ritz, K., Waine, T., 2012. Indicators of soil quality - physical properties (SP1611). Final report to DEFRA. Cranf. Univ. 1–45.
Rodionov, A., Welp, G., Damerow, L., Berg, T., Amelung, W., Pätzold, S., 2015. Towards on-the-go field assessment of soil organic carbon using Vis–NIR diffuse reflectance spectroscopy: Developing and testing a novel tractor-driven measuring chamber. Soil and Tillage Res. 145, 93–102. https://doi.org/10.1016/j.still.2014.08.007.
Roudier, P., 2011. clhs: Conditioned latin hypercube sampling. R package version 0.9.0.
Sanderman, J., Savage, K., Dangal, S.R., 2020. Mid-infrared spectroscopy for prediction of soil health indicators in the United States. Soil Sci. Soc. Am. J. 84 (1), 251–261. https://doi.org/10.1002/saj2.20009.
Sanderman, J., Gholizadeh, A., Pittaki-Chrysodonta, Z., Huang, J., Safanelli, J.L., Ferguson, R., 2023. Transferability of a large mid-infrared soil spectral library between two Fourier-transform infrared spectrometers. Soil Sci. Soc. Am. J. 87 (3), 586–599. https://doi.org/10.1002/saj2.20513.
Sankey, J.B., Brown, D.J., Bernard, M.L., Lawrence, R.L., 2008. Comparing local vs. global visible and near-infrared (VisNIR) diffuse reflectance spectroscopy (DRS) calibrations for the prediction of soil clay, organic C and inorganic C. Geoderma, 148 (2), pp.149-158. Doi: 10.1016/j.geoderma.2008.09.019.
Santra, P., Sahoo, R.N., Das, B.S., Samal, R.N., Pattanaik, A.K., Gupta, V.K., 2009. Estimation of soil hydraulic properties using proximal spectral reflectance in visible,

near-infrared, and shortwave-infrared (VIS–NIR–SWIR) region. Geoderma 152 (3–4), 338–349. https://doi.org/10.1016/j.geoderma.2009.07.001.
Sarathjith, M.C., Das, B.S., Wani, S.P., Sahrawat, K.L., 2016. Variable indicators for optimum wavelength selection in diffuse reflectance spectroscopy of soil samples. Geoderma 267, 1–9. https://doi.org/10.1016/j.geoderma.2015.12.031.
Sarkar, D., Haldar, A., 2005. Physical and chemical methods in soil analysis: fundamental concepts of analytical chemistry and instrumental techniques. New Age. International.
Savitzky, A., Golay, M.J., 1964. Smoothing and differentiation of data by simplified least squares procedures. Anal. Chem. 36, 1627–1639.
Sendhil, R., Kumar, A., Sharma, A.K., Jasrotia, P., Gupta, O.P., Meena, R.P., Singh, S., Singh, G.P., 2018. Strengthening value chain in wheat and barley for doubling farmers income. Directorate of Extension, Department of Agriculture Cooperation & Farmers Welfare and ICAR-Indian Institute of Wheat and Barley Research, pp.1–144.
Sharma, R.S., Mondal, M.E.A., 2019. Evolution of the Indian Shield: A new Approach. In: Mondal, M. (Ed.), Geological Evolution of the Precambrian Indian Shield. Society of Earth Scientists Series, Springer, pp. 17–38.
Shepherd, K.D., Walsh, M.G., 2002. Development of reflectance spectral libraries for characterization of soil properties. Soil Sci. Soc. Am. J. 66 (3), 988–998. https://doi.org/10.2136/sssaj2002.9880.
Shepperd, M., MacDonell, S., 2012. Evaluating prediction systems in software project estimation. Informat. Software Technol. 54 (8), 820–827. https://doi.org/10.1016/j.infsof.2011.12.008.
Shi, Z., Ji, W., Viscarra Rossel, R.A., Chen, S., Zhou, Y., 2015. Prediction of soil organic matter using a spatially constrained local partial least squares regression and the Chinese vis-NIR spectral library. Eur. J. Soil Sci. 66, 679–687. https://doi.org/10.1111/ejss.12272.
Silhavy, P., Silhavy, R., Prokopova, Z., 2021. Spectral clustering effect in software development effort estimation. Symmetry 13 (11), 2119. https://doi.org/10.3390/sym13112119.
Singh, R., Akuraju, V., Anantha, K.H., Garg, K.K., Barron, J., Whitbread, A.M., Dev, I., Dixit, S., 2022. Traditional rainwater management (haveli cultivation) for building system level resilience in a fragile ecosystem of Bundelkhand Region, Central India. Front. Sustain. Food Syst. 6, 826722 https://doi.org/10.3389/fsufs.2022.826722.
Singh, K., Vasava, H.B., Snoeck, D., Das, B.S., Yinil, D., Field, D., Sanderson, T., Fidelis, C., Majeed, I., Panigrahi, N., 2019. Assessment of cocoa input needs using soil types and soil spectral analysis. Soil Use Manag. 35 (3), 492–502. https://doi.org/10.1111/sum.12499.
Stevens, A., Ramirez-Lopez, L., 2022. An introduction to the prospectr package. R package Vignette R package version 0.2.6. https://cran.r-project.org/web/packages/prospectr/vignettes/prospectr.html.
Sudduth, K.A., Hummel, J.W., 1996. Geographic operating range evaluation of a NIR soil sensor. Trans. ASAE 39 (5), 1599–1604. https://doi.org/10.13031/2013.27674.
Tian, Y., Zhang, J., Yao, X., Cao, W., Zhu, Y., 2013. Laboratory assessment of three quantitative methods for estimating the organic matter content of soils in China based on visible/near-infrared reflectance spectra. Geoderma 202, 161–170. https://doi.org/10.1016/j.geoderma.2013.03.018.
Tsatsoulis, T., Tsakiridis, N.L., Karyotis, K., Zalidis, G.C., 2023, October. Transferability of Machine Learning Models for Soil Properties on Lucas Topsoil Spectral Libraries. In 2023 13th Workshop on Hyperspectral Imaging and Signal Processing: Evolution in Remote Sensing (WHISPERS) (pp. 1-5). IEEE. https://doi.org/10.1109/WHISPERS61460.2023.10431045.
UNCCD, 2016. Report of the Conference of the Parties on its twelfth session, held in Ankara from 12 to 23 October 2015. Part two: Actions. ICCD/COP(12)/20/Add.1. United Nations Convention to Combat Desertification (UNCCD), Bonn. http://www.unccd.int/Lists/OfficialDocuments/cop12/20add1eng.pdf.
Viscarra Rossel, R.A., McBratney, A.B., 2008. Diffuse Reflectance Spectroscopy as a Tool for Digital Soil Mapping. In: Hartemink, A.E., McBratney, A., Mendonça-Santos, M.d. (Eds), Digital Soil Mapping with Limited Data. Springer, Dordrecht. Doi: 10.1007/978-1-4020-8592-5_13.
Viscarra Rossel, R.A., Walvoort, D.J.J., McBratney, A.B., Janik, L.J., Skjemstad, J.O., 2006. Visible, near infrared, mid infrared or combined diffuse reflectance spectroscopy for simultaneous assessment of various soil properties. Geoderma 131 (1–2), 59–75. https://doi.org/10.1016/j.geoderma.2005.03.007.
Viscarra Rossel, R.A., Behrens, T., Ben-Dor, E., Brown, D.J., Demattê, J.A.M., Shepherd, K.D., Shi, Z., Stenberg, B., Stevens, A., Adamchuk, V., Aïchi, H., 2016. A global spectral library to characterize the world's soil. Earth Sci. Rev. 155, 198–230. https://doi.org/10.1016/j.earscirev.2016.01.012.
Viscarra Rossel, R.A., Behrens, T., Ben-Dor, E., Chabrillat, S., Demattê, J.A.M., Ge, Y., Gomez, C., Guerrero, C., Peng, Y., Ramirez-Lopez, L., Shi, Z., 2022. Diffuse reflectance spectroscopy for estimating soil properties: a technology for the 21st century. Eur. J. Soil Sci. 73 (4), e13271.
Viscarra Rossel, R.A., Shen, Z., Lopez, L.R., Behrens, T., Shi, Z., Wetterlind, J., Sudduth, K.A., Stenberg, B., Guerrero, C., Gholizadeh, A., Ben-Dor, E., 2024. An imperative for soil spectroscopic modelling is to think global but fit local with transfer learning. Earth-Sci. Rev., 104797 https://doi.org/10.1016/j.earscirev.2024.104797.
Viscarra Rossel, R.A., Webster, R., 2012. Predicting soil properties from the Australian soil visible–near infrared spectroscopic database. Eur. J. Soil Sci. 63 (6), 848–860. https://doi.org/10.1111/j.1365-2389.2012.01495.x.
Walkley, A., Black, I.A., 1934. An examination of the Degtjareff method for determining soil organic matter, and a proposed modification of the chromic acid titration method. Soil Sci. 37 (1), 29–38.
Wan, M., Qu, M., Hu, W., Li, W., Zhang, C., Cheng, H., Huang, B., 2019. Estimation of soil pH using PXRF spectrometry and Vis-NIR spectroscopy for rapid environmental risk assessment of soil heavy metals. Process Safety Environ. Protect. 132, 73–81. https://doi.org/10.1016/j.psep.2019.09.025.
Wandrey, C.J., Law, B.E., 1997. Open-File Report 97-470C. US Geological Survey Open File Report, 97, p.470C.
Wang, J., Cui, L., Gao, W., Shi, T., Chen, Y., Gao, Y., 2014. Prediction of low heavy metal concentrations in agricultural soils using visible and near-infrared reflectance spectroscopy. Geoderma 216, 1–9. https://doi.org/10.1016/j.geoderma.2013.10.024.
Wang, Q., Li, P., Chen, X., 2012. Modeling salinity effects on soil reflectance under various moisture conditions and its inverse application: a laboratory experiment. Geoderma 170, 103–111. https://doi.org/10.1016/j.geoderma.2011.10.015.
Wang, L., Wang, R., 2022. Determination of soil pH from Vis-NIR spectroscopy by extreme learning machine and variable selection: A case study in lime concretion black soil. Spectrochim. Acta Mol. Biomol. Spectrosc. 283, 121707 https://doi.org/10.1016/j.saa.2022.121707.
Wetterlind, J., Stenberg, B., 2010. Near-infrared spectroscopy for within-field soil characterization: small local calibrations compared with national libraries spiked with local samples. Eur. J. Soil Sci. 61 (6), 823–843. https://doi.org/10.1111/j.1365-2389.2010.01283.x.
Wu, J., Jones, K.B., Loucks, O.L. (Eds.), 2006. Scaling and Uncertainty Analysis in Ecology. Springer, Netherlands.
Xu, S., Zhao, Y., Wang, Y., 2024. Optimizing machine learning models for predicting soil pH and total P in intact soil profiles with visible and near-infrared reflectance (VNIR) spectroscopy. Comput. Electron. Agricult. 218, 108643 https://doi.org/10.1016/j.compag.2024.108643.
Yang, M., Chen, S., Xu, D., Hong, Y., Li, S., Peng, J., Ji, W., Guo, X., Zhao, X., Shi, Z., 2023. Strategies for predicting soil organic matter in the field using the Chinese Vis-NIR soil spectral library. Geoderma 433, 116461. https://doi.org/10.1016/j.geoderma.2023.116461.
Zayani, H., Fouad, Y., Michot, D., Kassouk, Z., Lili-Chabaane, Z., Walter, C., 2023. Detecting the temporal trend of cultivated soil organic carbon content using visible near infrared spectroscopy. J. near Infrar. Spectrosc. 31 (5), 241–255. https://doi.org/10.1177/09670335231193113.
Zeng, R., Rossiter, D.G., Zhang, J., Cai, K., Gao, W., Pan, W., Zeng, Y., Jiang, C., Li, D., 2022. How well can reflectance spectroscopy allocate samples to soil fertility classes? Agronomy 12 (8), 1964. https://doi.org/10.3390/agronomy12081964.
Zhao, X., Zhao, D., Wang, J., Triantafilis, J., 2022. Soil organic carbon (SOC) prediction in Australian sugarcane fields using Vis–NIR spectroscopy with different model setting approaches. Geoder. Regl. 30, e00566.
Zhao, X., Wang, J., Koganti, T., Triantafilis, J., 2024. Developing Vis–NIR libraries to predict cation exchange capacity (CEC) and pH in Australian sugarcane soil. Comput. Electron. Agricult. 221, 109004 https://doi.org/10.1016/j.compag.2024.109004.